EUROPEAN COMMISSION
Community Research

SEVENTH FRAMEWORK PROGRAMME

CARBOWASTE

Treatment and Disposal of Irradiated Graphite and Other Carbonaceous Waste

Grant Agreement Number: FP7-211333

Deliverable (D.4.1.3)

Final report on the relationships between structure and isotope distribution in graphite

Author(s): Abbie Jones; Greg Black & Lorraine McDermott

University of Manchester,

Werner von Lensa, Dirk Vulpius;
Forschungszentrum Juelich GmbH

Reporting period: 01/04/2008– 31/01/2013

Date of issue of this Report:

Start date of project: **01/04/2008** Duration: **60 Months**

Distribution list

Person and organisation name and/or group	Comments
Mr G. Black	
Dr A N Jones	
Task 4.1 members	
Executive Board	
Co-ordinator	

CARBOWASTE		
Work package: 4 **Deliverable: :** 4.1.3 (and T4.1.1 & T4.1.2)	**CARBOWASTE document no:** Deliverable 4.1.3	**Document type:** Deliverable
Issued by: UoM **Internal no.:** UoM_WP3_D4.1.3 _Final		**Document status:** Final

Project co-funded by the European Commission under the Seventh Framework Programme (2007 to 2011) of the European Atomic Energy Community (EURATOM) for nuclear research and training		
Dissemination Level		
PU	Public	
RE	Restricted to the partners of the CARBOWASTE project	**X**
CO	Confidential, only for specific distribution list defined on this document	

Document title
Final report on the relationships between structure and isotope distribution in graphite
Executive summary

This final report builds on analysis of data for the various grades of unirradiated and irradiated graphite obtained in WP3 in conjunction with data obtained for the treated graphite in WP4. This combines Tasks 4.1.1 (Indicative relationships between structure and isotope distribution in graphite) and 4.1.2 (Interim report on the relationships between structure and isotope distribution in graphite) for the Deliverable.

The mechanistic background of impurity / isotope localisation before and after treatment is required to feed into the treatment options within WP4 and subsequent work packages. A literature review has been undertaken to investigate the mechanistic background of impurity content and removal from irradiated graphite waste. The process involved in predicting the end of life radionuclide inventory has been identified and research has been undertaken in order to apply this to a statistical model for impurity removal. Techniques such as Autoradiography and X-ray tomography have also been highlighted for the analysis of impurity and isotopic location within the graphite. A fundamental understanding of radionuclide origins, removal mechanisms, combined with the development of improved graphite purification methods, may enable the manufacture of new grades of nuclear graphite with lower impurity concentrations, being important for both improved neutronics and waste minimisation. In addition a meeting was held at the university of Manchester on the 28th November 2012 in order to bring together specialists in the fields of irradiation damage, atomistic modelling, experimental nano-structural methods and inventory modelling, to discuss the problem of irradiation damage and 14C formation in Nuclear Graphite. This was a joint meeting in conjunction with the FP7 CARBOWASTE programme and the presentations and minutes of which are highlighted in this deliverable.

Revisions						
Rev.	Date	Short description	Author	Internal Review	Task Leader	WP Leader
00	8th Feb 2013	Draft Reviewed	*ANJ*	ANJ	ANJ	DV
01						

Table of Contents

1 Introduction

The radionuclide content of irradiated graphite from nuclear reactor cores can arise from two sources: intrinsic and extrinsic. Intrinsic radioactivity results from the neutron activation of carbon and other stable impurities within the graphite structure [1]. Extrinsic radioactivity is the result of surface contamination from other components in the reactor circuit due to damage and corrosion; possible sources include fuel cladding, the pressure vessel, coolant gas and various other support structures [2]. In some cases this contribution can be relatively large, as for AGRs which have been contaminated with cobalt containing metal oxides within the reactor circuit leading to a significant further Co-60 contribution [2]. An additional source of radioactivity, which may be of either an intrinsic or extrinsic origin, are fission products which will arise from both the fuel and the natural uranium impurity of the graphite (below 0.1ppm [2, 3]) when undergoing fission [2]. The origin of the radionuclides will therefore determine the location; an extrinsic origin will give rise to surface bound adsorped radionuclides whereas an intrinsic origin will result in the radionuclide being 'trapped' either interstially or intercalated inside the graphite structure.

It may be possible, through the application of various treatment techniques [4-6] to remove the surface radionuclides without compromising the structural integrity of the graphite, however any radionuclides which are located within the graphite structure will only be removed through the application of destructive techniques [7]. Thus the quantification of the impurity content of the graphite is an important factor in determining not only the end of life radioactivity of the graphite as well as the location, and therefore, the necessary treatment regime required to remove these.

1.1 Origin of impurities

The manufacturing process for nuclear grade graphite may include supplementary baking and reimpregnation steps [1, 8] to ensure the purity of the material. It is impossible to remove all the impurity content, in addition the purification process will also result in the introduction of impurity elements such a halogen (Cl or more recently F) gas [1]. Accurate information regarding the impurity inventory of nuclear graphite grades is limited, however various studies have shown that impurities levels are relatively low and measured in parts-per-million (ppm) [3]. One such study was performed by White et al, 1984 [3], which experimental determined the impurity content of the graphite grades used in the UK Magnox and AGR class of reactors; the results of which are detailed in Table 1.

Table 1: Reference Graphite impurity levels [3]

Element	Magnox (ppm)	AGR (ppm)	Element	Magnox (ppm)	AGR (ppm)
Li	0.05	0.05	Ni	1.0	6.0
Be	0.02	0.02	Zn	0.13	1.0
B	0.1	0.5	Sr	0.4	0.4
N	10	10	Mo	0.1	2.5
Na	1.0	4.0	Ag	0.001	0.001
Mg	0.1	0.4	Cd	0.04	0.07
Al	1.0	4.0	In	0.05	0.06
Si	35	35	Sn	0.05	1.0
S	50	60	Ba	1.5	0.5
Cl	2.0	4.0	Sm	0.04	0.05
Ca	35	25	Eu	0.004	0.005
Ti	3	0.7	Gd	0.005	0.01
V	12	0.4	Dy	0.008	0.006
Cr	0.35	0.4	W	0.12	0.15

Element	Magnox (ppm)	AGR (ppm)	Element	Magnox (ppm)	AGR (ppm)
Mn	0.04	0.25	Pb	0.12	0.8
Fe	10	28	Bi	0.08	0.05
Co	0.02	0.7	Ni	1.0	6.0

1.2 Activation Inventory Products

White et al (1984) then performed a simulation, using the United Kingdom Atomic Energy Agency (UKAEA) FISPIN© software (a nuclide inventory calculation code) to calculate the resultant radionuclides from the impurities in Table 1 after a reactor lifetime of 40 years followed by 10 years storage time. The calculated results for reference Magnox and AGR reactors are given in Table 2.

Table 2: Activation inventory for reference Magnox (2233tonnes of graphite) and AGR (1633tonnes of graphite) [from [2]]

Radionuclide	Magnox (Bq)	AGR (Bq)	Radionuclide	Magnox (Bq)	AGR (Bq)
H-3	1.2×10^{14}	7.6×10^{13}	Mo-93	8.5×10^{8}	8.5×10^{10}
Be-10	7.1×10^{10}	2.3×10^{11}	Nb-93m	5.5×10^{8}	3.4×10^{10}
C-14	8.5×10^{13}	1.9×10^{14}	Nb-94	1.0×10^{5}	8.4×10^{6}
Cl-36	9.5×10^{11}	2.3×10^{12}	Tc-99	1.7×10^{8}	5.6×10^{9}
Ca-41	7.3×10^{11}	1.2×10^{12}	Ag-108m	2.3×10^{10}	3.6×10^{10}
Mn-54	2.7×10^{8}	5.2×10^{9}	Cd-113m	1.0×10^{10}	4.4×10^{10}
Fe-56	1.5×10^{13}	9.3×10^{13}	Sn-121m	4.5×10^{10}	2.8×10^{12}
Ni-59	9.3×10^{10}	5.5×10^{11}	Ba-133	5.6×10^{11}	3.1×10^{11}
Co-60	2.7×10^{13}	9.8×10^{14}	Eu-152	2.2×10^{11}	1.0×10^{11}
Ni-63	1.3×10^{13}	1.1×10^{14}	Eu-154	2.2×10^{12}	2.9×10^{12}
Zn-65	2.1×10^{8}	3.7×10^{9}	Eu-155	1.6×10^{12}	9.4×10^{11}

From these activation products the beta emitting C-14 ($t_{1/2}$ = 5730 y), H-3 ($t_{1/2}$ = 12.32 y) and Cl-36 ($t_{1/2}$ = 301,000 y) isotopes are considered to represent the most likely contaminates to the food chain, and gamma emitting nuclides including Co-60 ($t_{1/2}$ = 5.2714 y), Nb-94 ($t_{1/2}$ = 20,300 y), Eu-152 ($t_{1/2}$ = 13.537 y) and Eu-154 ($t_{1/2}$ = 8.593 y) will present a risk to dismantling, handling and storage operations [2]. In order to quantify the final activity of individual radioisotopes it is important to consider the routes from which these are generated, for example Carbon-14 is produced by a variety of routes, the dominant ones identified as: $^{14}N(n,p)^{14}C$, $^{13}C(n,\gamma)^{14}C$ and $^{17}O(n,\alpha)^{14}C$. The contribution per route is related to both the reaction-cross section and the precursor elemental concentration (both as a virgin impurity and contaminates). There is currently a debate within the scientific community to the significance of each production route and their contributions to final carbon-14 content, it is hoped that work within the Carbowaste WP4 program will provide an insight into these mechanisms and the dominance.

Tritium (H-3) also has a variety of production routes the main contribution estimated to be from neutron activation of the Li impurity, through the (n, p) reaction [9, 10] with additional production pathways from Boron and Nitrogen (both present as impurities in the core). Chlorine-36 may arise from the activation of Chlorine impurities within the graphite which are present as a result of its use during purification of the graphite [11].

The contribution to the radionuclide inventory from the fission of uranium fuel and impurity was also calculated; the results are given in Table 3.

Table 3: Inventory (Bq) for irradiation of 0.1ppm natural Uranium in reference Magnox & AGR (40 years lifetime operation followed by 10 years decay) [from [2]]

Magnox				AGR			
Se-79	1.80×10^{6}	Eu-152	3.19×10^{7}	Se-79	2.98×10^{6}	Eu-152	2.53×10^{7}
Sr-90/Y-90	1.36×10^{11}	Eu-154	1.87×10^{10}	Sr-90/Y-90	2.05×10^{11}	Eu-154	3.54×10^{10}
Kr-85	6.44×10^{9}	Eu-155	6.59×10^{9}	Kr-85	1.05×10^{9}	Eu-155	1.50×10^{9}
Zr-93	1.30×10^{7}	U-236	5.33×10^{5}	Zr-93	2.07×10^{7}	U-236	3.29×10^{5}
Nb-93m	1.00×10^{7}	U-238	2.68×10^{6}	Nb-93m	1.57×10^{7}	U-238	1.89×10^{6}
Tc-99	6.67×10^{7}	Np-237	8.26×10^{5}	Tc-99	9.04×10^{7}	Np-237	1.49×10^{5}
Ru-106/Rh-106	4.19×10^{8}	Pu-238	3.53×10^{10}	Ru-106/Rh-106	8.52×10^{8}	Pu-238	4.07×10^{10}
Pd-107	1.04×10^{6}	Pu-239	1.09×10^{9}	Pd-107	2.19×10^{6}	Pu-239	1.09×10^{9}
Cd-113m	6.41×10^{7}	Pu-240	2.28×10^{9}	Cd-113m	1.37×10^{7}	Pu-240	2.13×10^{9}
Sb-125	7.11×10^{8}	Pu-241	3.30×10^{11}	Sb-125	1.37×10^{8}	Pu-241	4.07×10^{11}
Te-125m	1.74×10^{8}	Pu-242	3.09×10^{7}	Te-125m	3.34×10^{8}	Pu-242	5.81×10^{7}
I-129	1.87×10^{5}	Am-241	1.18×10^{10}	I-129	3.31×10^{5}	Am-241	1.14×10^{10}
Cs-134	6.96×10^{9}	Am-243	3.22×10^{8}	Cs-134	2.50×10^{9}	Am-243	1.09×10^{8}
Cs-135	5.74×10^{6}	Cm-244	2.21×10^{10}	Cs-135	8.44×10^{6}	Cm-244	3.47×10^{10}
Cs-137	2.99×10^{11}	Cm-245	3.24×10^{6}	Cs-137	5.52×10^{11}	Cm-245	2.40×10^{6}
Ce-144	4.96×10^{7}	Cm-246	1.62×10^{6}	Ce-144	9.48×10^{7}	Cm-246	3.50×10^{6}
Sn-126	3.70×10^{6}			Sn-126	7.15×10^{6}		
Pm-147	1.26×10^{10}			Pm-147	1.70×10^{10}		
Sm-151	5.56×10^{8}			Sm-151	8.48×10^{8}		

The yields of the radionuclides outlined in Table 3 are generally low compared with those from other impurities (Table 2) with the exception of Cs-137 [2].

2 Impurity and isotopes analysis

2.1 Autoradiography

Autoradiography provides a visual distribution of radiation present in the surface of a sample, depending on isotope energy [12, 13]. Autoradiography can therefore determine β and γ radiation present within nuclear graphite with energy above 0.018MeV. Weak β-emitting isotopes and α isotopes are stopped by the coating on the phosphorous storage film (recording medium). Autoradiography is a qualitative technique used to analyse high energy β and γ isotopes present within a nuclear graphite sample.

The phosphor storage screens comprise of fine crystals of $BaFBr:Eu^{+2}$ in an organic binder. Upon exposure to radiation the Eu^{+2} is excited to the oxidised Eu^{+3} state and the BaFBr is reduced to $BaFBr^{-}$. The phosphor storage screen releases this energy when exposed to light of an appropriate wavelength. Excited electrons fall to the ground state thus releasing energy in the form of blue light. The emitted light passes through a photomultiplier detector which converted to produce an electric current proportional to the activity in the sample.
The advantages of this technique include reduced exposure time compared to traditional autoradiography using X-ray film and increased sensitivity with a linear dynamic range of 1 to 100000 which allows both weak and strong energy isotopes to be analysed simultaneously.

2.2 Autoradiography Analysis at the UoM

A Typhoon 9410 Amersham instrument has been used throughout this study. Sample size, or preferentially diameter is shown to have significant effect on the autoradiography results. Autoradiography analysis of graphite samples thicker than 1cm have proved difficult to

analyse with the high energy radionuclide's saturating the film after only a 4 - 6 hours, making comparison between graphite samples that have acquired varying levels of dose or exposure inconclusive.

In total 60 samples have been analysed. The sample size was 1mm in diameter. The autoradiography screen was wiped clean after each use using a light box and a lint free cloth. The samples were placed on the screen in a glove box and left for 20 hours. This length of time was determined as sufficient exposure time without saturating the film due to the activity present in the graphite and will vary for each type of sample being analysed.

Analysis of the film performed using the Amersham (wavelength of 633nm) and a pixel size of 50 microns. The average intensity, standard deviation, variance, minimum and maximum intensity and area are calculated. This allows the background to be deducted from analysis and documents any errors between results.

Autoradiography was carried out on all BEPO samples in order to gain a qualitative assessment of the distribution of radioisotopes within the irradiated BEPO material. Figure 2 shows the average intensity of the samples with increasing sample numbers after an exposure time of 20 hours. Sample 1 exhibits the least intensity of the BEPO materials, which corresponds to the least active samples, there is a non-uniform distribution of radioisotopes which can be noted by the presence of high intensity regions contained within sample 16, this is also a high distribution of activity with both sample 20 and 21 this film is fully saturated and again shows a non-uniform disruption of β and γ activity within the sample.

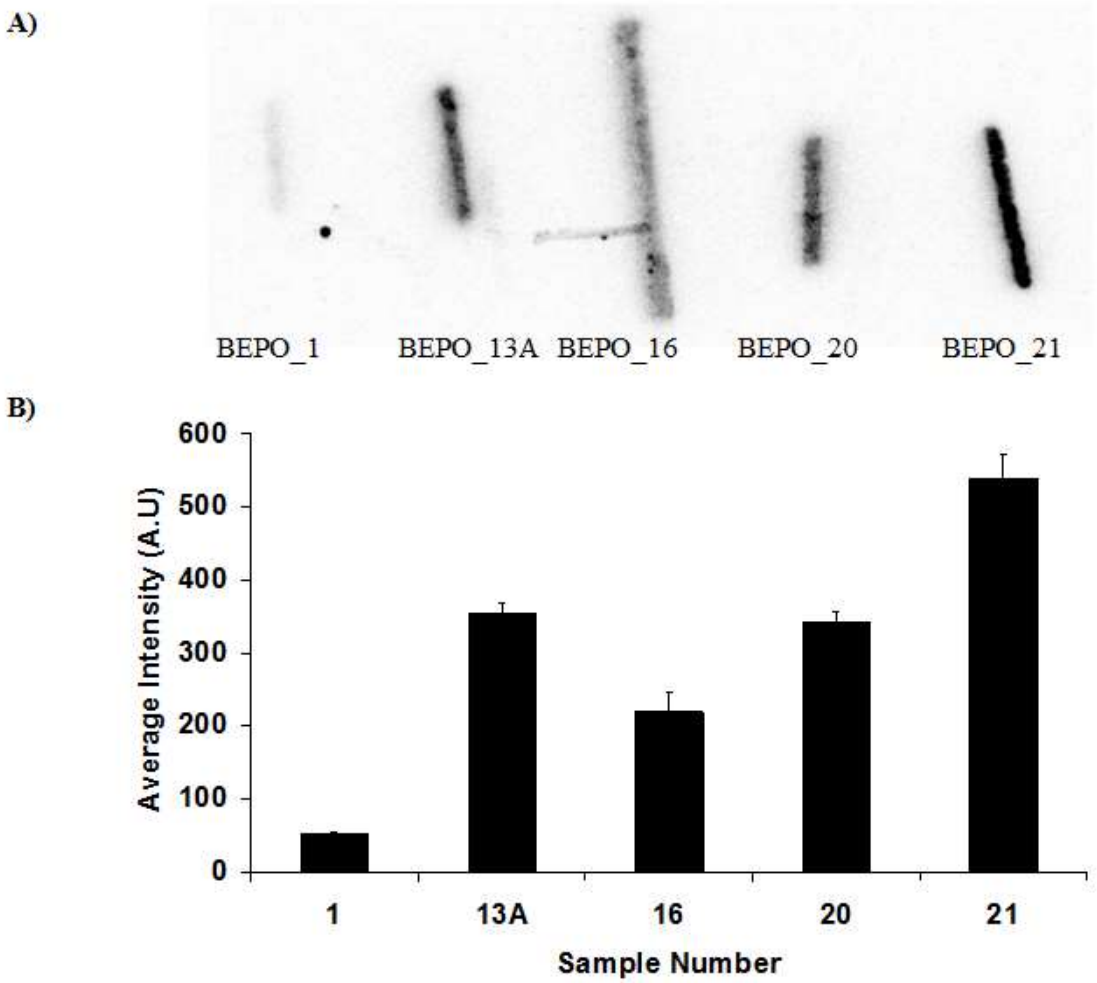

Figure 1: Autoradiograph showing increasing greyscale intensities with exposed BEPO samples, B) graph showing the average intensity for BEPO samples.

These results can be compared with similar analysis performed on a set of samples from the Oldbury Reactor 2. These samples are PGA graphite and were placed in a sample holder during the commissioning of the reactor in 1967 and removed in 2005; samples conditions are given in Table 4. Autoradiography results are shown in Figure 2.

Table 4: Oldbury installed samples irradiation history

Irradiation conditions	
Irradiation temperature (˚C)	269
Adjacent fuel dose / (MWd/t	52827

DIDO equivalent dose at channel wall / 10^{20} n/cm^2	40.27
DPA	5.28

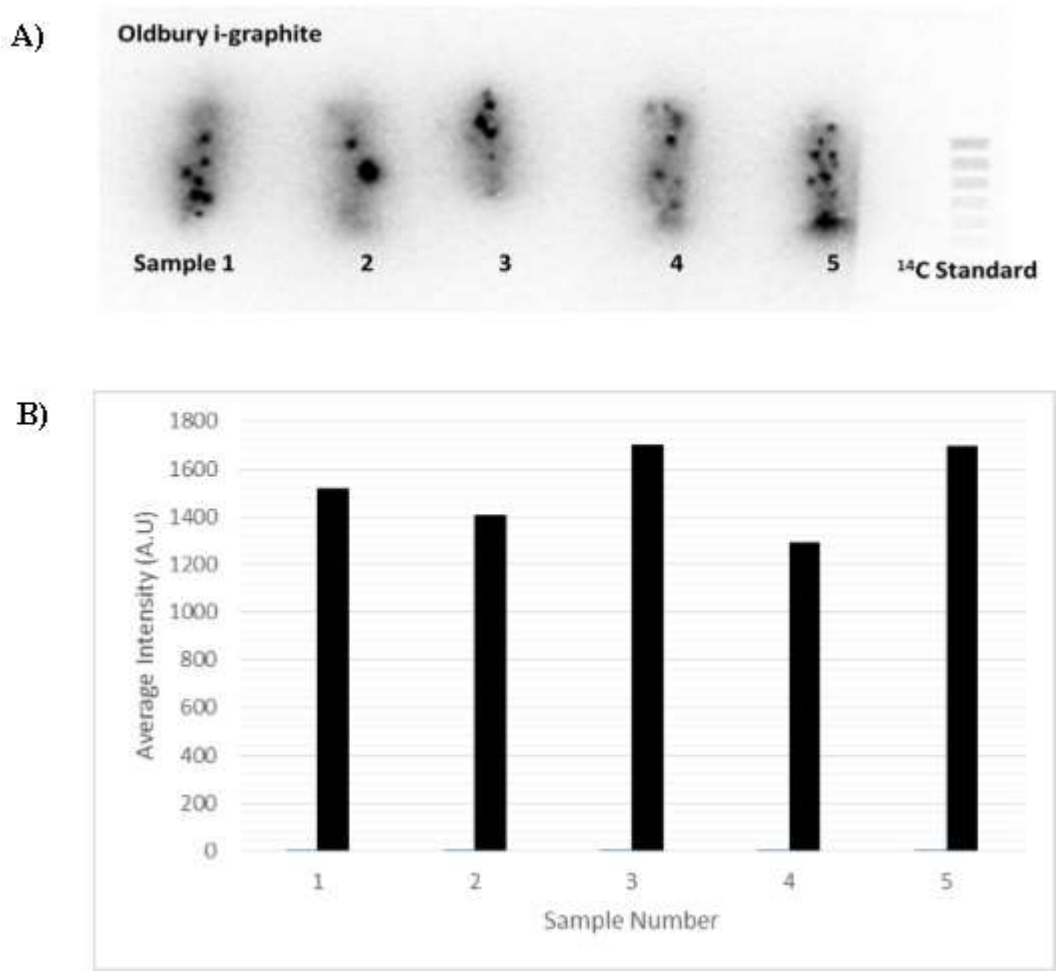

Figure 2: Autoradiograph showing increasing greyscale intensities with exposed Oldbury samples, B) graph showing the average intensity for Oldbury samples.

2.3 X-ray Tomography

Computerised x-ray tomography is a non-destructive technique that allows the 3D microstructure of irradiated graphite to be analysed. This technique involves sending an X-

ray beam thorough the material and recording the transmitted beam using a charged coupled device camera as shown in Figure 3. The ratio of transmitted to incident photons is related to the integral of the absorption coefficient of the material along the path that the photons made through the material. Using an empirical law, the absorption coefficient can be related to the density, the atomic number and in certain cases, the energy [14-16]. The resulting radiograph is a projection of a volume in a given 2D plane. The method of acquiring a 3D image is to obtain radiographs whilst rotating the sample between 0° and 180°. An algorithm (filtered back-projection) is applied to reconstruct the volume from the 2D radiographs.

This CT data was used to determine porosity and density of the BEPO graphite. The smallest porosity or characteristics that can be identified however are limited to the resolution of the 2D radiographs which is determined by the sample size and CCD camera used.

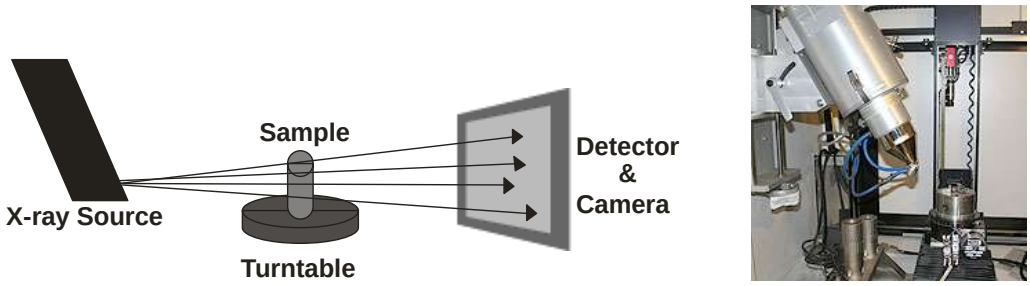

Figure 3. A) Schematic and B) photograph of X-ray tomography scanner;

2.4 X-ray Tomography Analysis at the UoM

Tomography images were collected using the X-TEK HMX CT instrument using the parameters outlined in Table 4. In addition, a rotation of 0.3º with 32 frames and a camera exposure time of 160s were also applied. A voxel size of 21.4 µm was resolved.

Irradiated graphite analysis was performed with the samples contained within a 'harwell can', this ensured that no radioactive graphite dust would contaminate the tomography equipment. No filter was applied during the analysis as the can is made from aluminium which acts as a filter. A calibration of the can's thickness versus attenuation using highly orientated pyrolytic graphite (HOPG) as a reference standard inside the can is shown in Figure 4 where intensity shown to exhibit a linear relationship with thickness. The reconstruction of the 2D images was completed using Amira© software and are shown in Figure 5.

Table 5: Tomography experimental parameters

Parameters	Settings
Target	Copper
Filter	None
Detector	Beryllium
Voltage	95 kV
Current	105 µA

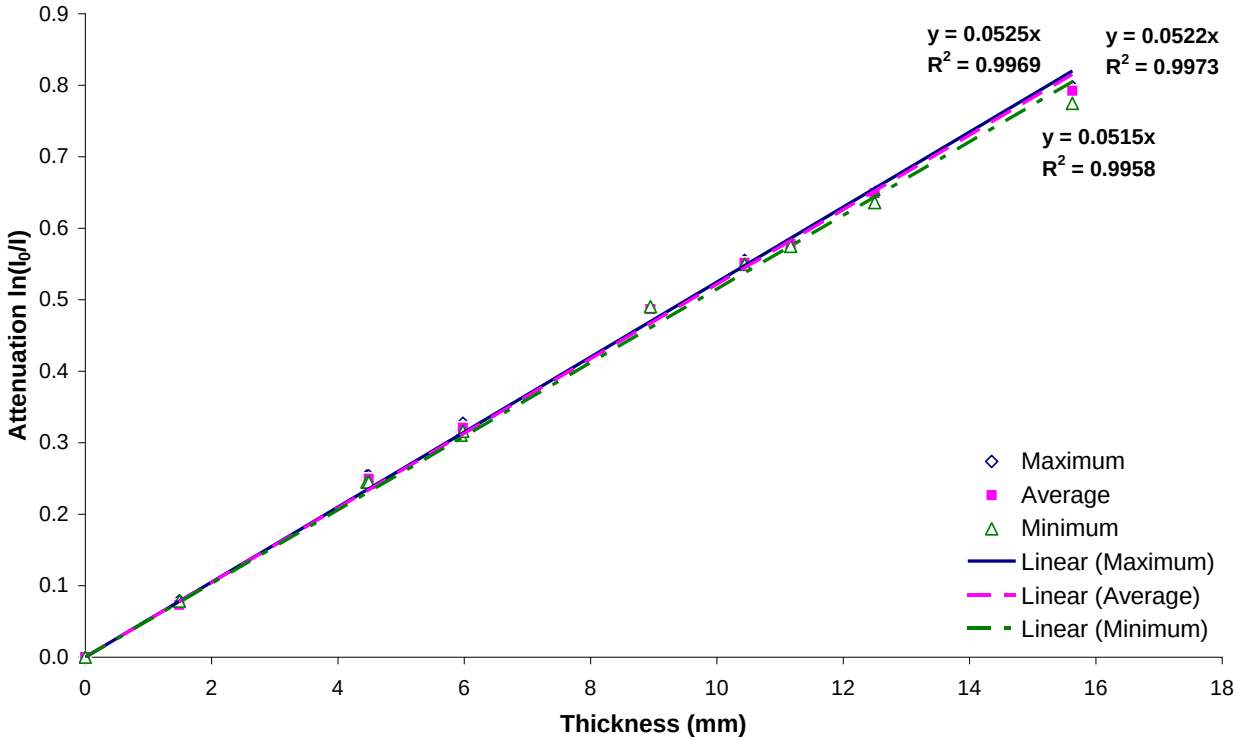

Figure 4: Calibration graph of thickness of HOPG sample inside a Harwell can versus the attenuation intensity of the transmitted incident photons that have passed through the HOPG sample.

2D slices of BEPO graphite with high attenuation were observed and are shown in Figure 5. These spots are of a material with a much higher density and therefore elemental number than that of graphite. The majority of these high attenuation spot are noted to be next to or contained within areas of porosity.

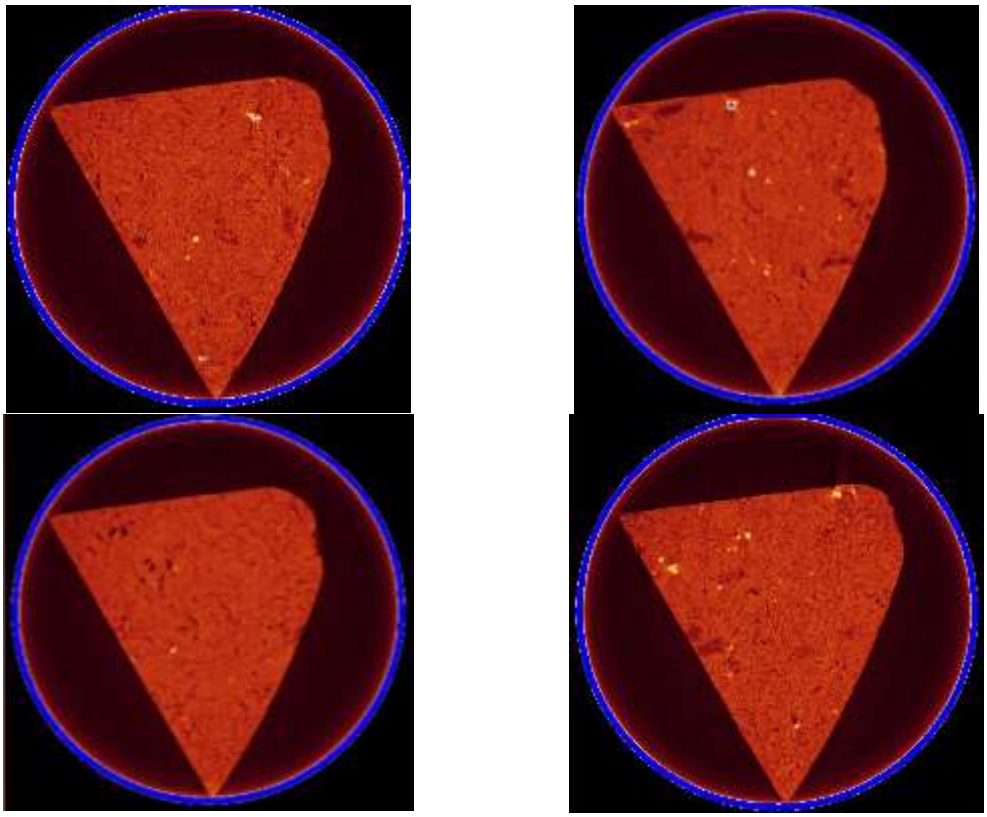

Figure 5: 2D tomography Radiographs of BEPO sample 16 graphite contained within a Harwall can.

3D volume reconstructions of BEPO sample 16 have been processed using Amira© software and are shown in Figure 6. The porosity distribution was calculated and is equivalent to 17.2% porosity. The blue regions display the internal porosity and the red is the high attenuation spots. It can be noted the is these high attenuations spots are contained within the porosity and are non uniformly distributed.

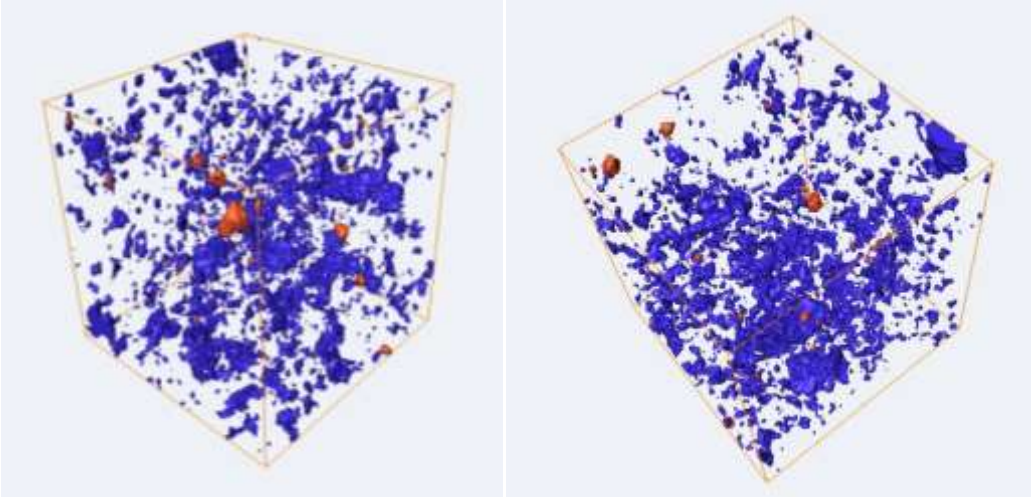

Figure 6: 3D volume reconstructions of BEPO Graphite using Amira© software

3 14C modelling meeting, Manchester 28/11/12

A meeting was held at the University of Manchester on the 28th November 2012. The aim of this meeting was to bring together experts in the fields of atomistic modelling, experimental analysis and neutronics/activation modelling. Work within the Carbowaste programme in WP3 has focused on simulating reactor neutron flux and using this information to perform activation modelling using a variety of codes. From this work it has been recognised that the production of 14C from both the original precursor elements in the graphite and as a result of coolant bound contaminants varies depending on the particular reactor system under investigation. This type of modelling does not provide information of the location of 14C within the graphite, which is important when developing treatment and decontamination procedures. The aim of the meeting held in Manchester was to engage experts in the field of atomistic modelling, providing information on the behaviour of the precursor 13C & 14N atoms and the resultant 14C atoms within the graphite matrix. In addition experts in experimental analysis techniques also contributed to highlight potential methods to validate the atomistic models. Finally the day ended with contributions from

WP3 participants from the UoM, NNL and LEI; ways forward were then discussed. The scope of the joint meeting and the areas of focus included:

- Location of activation products
- Chemical speciation of activation products
- Temperature induced migration of activation products
- Agglomeration of activation products at pore surfaces/grain boundaries
- Impact of radiolytic corrosion on release of activation products
- Structural change of irradiated graphite by irradiation

The agenda and abstracts are given in the following sections and copies of the presentations are provided in Appendix 1, presentations not released by the authors may be discussed directly by contacting the relevant individual. An additional speaker (not identified on the agenda), Prof. R. Nabbi from Aachen University presented: '*Molecular dynamic simulation of the transport behaviour of C-14 in irradiated graphite'*.

3.1 Agenda

8.30	Arrival - Tea & coffee available in the 2nd floor common room	
9.15	Welcome and introduction	Abbie Jones / Barry Marsden The University of Manchester
9.30	Carbowaste project and 14C Formation	Werner von Lensa Carbowaste co-ordinator, FZJ
10.00	Displacement damage in graphite – guidance from first principles and from the literature	Malcolm Heggie, University of Surrey
10.30	Nanostructure of Pyrocarbon Matrices: from experimental characterizations to atomistic models	Jean-Marc Leyssale CNRS, France
11.00	Coffee Break	

11.20	In situ ion irradiation of graphite	Steve Donnelly, University of Huddersfield
11.50	Synergistic or decoupled effects of temperature and irradiation on ^{14}C and ^{36}Cl behavior in irradiated graphite studied through ion implantation or irradiation of virgin nuclear graphite	Nelly Toulhoat, Université de Lyon
12.20	The Use of Small Angle Neutron Scattering in the Study of Porosity in Nuclear Graphite:	Keith Ross University of Salford
12.50	Discussions	
1.00	Lunch	
2.00	Irradiation Damage of Graphite in-reactor and its Disposal	John Lillington AMEC
2.30	Understanding Carbon-14 production in UK Magnox reactors by activation modelling and mass balance studies	Martin Metcalfe NNL
3.00	Modelling of C-14 production in irradiated graphite of RBMK–1500 reactors and comparison with experimental data	Ernastas Narkunas LEI, Lithuania
3.30	Radionuclide inventory determination for UK irradiated graphite wastes	Greg Black The University of Manchester
4.00	Tea /Coffee break	
4.15	Ways forward open discussion	
5.00	Close of meeting	

3.2 Abstracts

MALCOLM HEGGIE

Displacement damage in graphite – guidance from first principles and from the literature

M. I. Heggie, Department of Chemistry, Faculty of Engineering and Physical Science, University of Surrey, Guildford, BN1 9QJ, UK

Neutron damage is largely accepted to be displacement damage resulting from neutron:nucleus elastic collisions and the ensuing cascade. Atomic displacement creates Frenkel pairs and after generation these either annihilate, or aggregate. They create various defects from dimers to prismatic interstitial loops, which may also feature prismatic screw dislocations. It has also been suggested that radiation damage produces basal slip and other consequent artefacts as well. These will be discussed, with evidence from the literature, taking data for energy changes and activation barriers from first principles calculation. The implications for ^{14}C displacement during formation will be raised.

JEAN-MARC LEYSSALE

Nanostructure of Pyrocarbon Matrices: from experimental characterizations to atomistic models

Low temperature laminar pyrocarbons (PyC) matrices are essential constituents of many high performance Carbon/Carbon composites found in aerospace, aeronautics and nuclear industries. These materials, prepared by chemical vapour deposition or infiltration techniques, are anisotropic graphitic carbons with a high degree of structural disorder. I will present the strategy we have developed to discriminate between different microstructural variants of these materials. It includes the preparation of the materials in bulk form, their characterization using many techniques (Raman spectrometry, HRTEM, XRD and neutron diffraction, etc…) and the production of atomistic structural models from a combination of image analysis of HRTEM images, synthesis of 3D HRTEM-like images and molecular dynamics simulation constrained by the 3D image. The resulting models of different

pyrocarbons (rough laminar, regenerated laminar and smooth laminar) will be presented in details and validated through comparison of experimental and simulated HRTEM images and neutron diffraction data in reciprocal (S(Q) and real space (G(r)).

S E DONNELLY

In-situ transmission electron microscopy studies of ion-beam induced radiation damage in graphite

As part of the EPSRC-funded consortium project on "Fundamentals of Current and Future Uses of Nuclear Graphite", we are using ion beams to simulate the effects of neutron damage on thin films of graphite and observing the damaging processes in-situ in a transmission electron microscope. The aim of the work, carried out using the MIAMI facility at the University of Huddersfield, is to attempt to understand the atomistic processes responsible for the dimensional changes known to occur in graphite under irradiation. The presentation will include a discussion of recent observations of stress build-up, dislocation generation and cracking in thin, monocrystalline graphite films irradiated to low damage fluences (≈ 0.1 DPA) using 60 keV Xe ions.

NELLY TOULHOAT

Synergistic or decoupled effects of temperature and irradiation on 14C and 36Cl behavior in irradiated graphite studied through ion implantation or irradiation of virgin nuclear graphite

N. Toulhoat[1, 2], N. Moncoffre[1], Y. Pipon[1, 3], N. Bérerd[1, 3], G. Silbermann[1], A. Blondel[1]

1 Université de Lyon, CNRS/IN2P3, Université Lyon 1, Institut de Physique Nucléaire de Lyon (IPNL), 4 rue Enrico Fermi, 69 622 Villeurbanne cedex, France

2 Commissariat à l'Energie Atomique CEA-DEN, Centre de Saclay, 91 191 Gif sur Yvette, France

3 Université de Lyon, Université Lyon 1, IUT Lyon 1, 43 bd du 11 novembre 1918, 69 622 Villeurbanne cedex, France

The French UNGG reactors will be dismantled. The reference outlet is a direct disposal. Alternative solutions are also investigated as partial decontamination to reduce the radioactive waste inventory. In any case, the inventory has to be clarified prior to disposal or treatment. Our main objective is to get information on ^{14}C, ^{36}Cl and ^{3}H behavior in graphite under reactor operating conditions and obtain data on their speciation and distribution in irradiated graphite. Using ion implantation (to simulate the radionuclides) and irradiation, the synergistic or independent effects of temperature, coolant gas radiolysis and graphite irradiation is studied on virgin graphite. We shall present our experimental approach as well as the main results already obtained on carbon and chlorine.

KEITH ROSS

The Use of Small Angle Neutron Scattering in the Study of Porosity in Nuclear Graphite:

D.K.Ross and Z. Mileeva

Centre for Material and Physics, School of Computing, Science and Engineering, University of Salford, M5 4WT

We report how the SANS technique, recently demonstrated for activated carbon[1] also offers unique information on porosity in graphite in the nm to μm length range. The remarkable result is that reactor graphites have a fractal distribution of pore sizes in the observed length scale but with a fractal dimension that is changed by either neutron irradiation or radiolytic oxidation. We have recently demonstrated that SANS decreases linearly with increasing temperature, showing that the porosity is largely due to the large thermal expansion in the c direction. By saturating the sample with deuterated toluene that matches the graphite scattering density, we have also demonstrated that about 60% of the total porosity is open to the surface.

[1] Z. Mileeva, D.K. Ross, D. Wilkinson, S.M. King, T.A. Ryan and H. Sharrock, "The use of small angle neutron scattering with contrast matching and variable adsorbate partial pressures in the study of porosity in activated carbons". Carbon (2012), http://dx.doi.org/10.1016/j.carbon.2012.06.046

JOHN LILLINGTON

Irradiation Damage of Graphite in-reactor and its Disposal

The presentation will focus on AMEC's contribution towards the understanding of graphite irradiation damage in-reactor and its disposal. It will start with a review of operational issues associated with the behaviour of graphite through life in the current Magnox and AGR reactor fleet. This will include a summary of the latest methodology for graphite stress analysis, its validation and mechanical testing experiments. Graphite dosimetry methods and their validation will also be described. The presentation will move on to cover legacy waste management of graphite, other carbonaceous waste and coated particle fuel from decommissioning of commercial, production and research reactors. It will conclude with a brief discussion on R & D to support future reactor, including Gen IV, designs.

MARTIN METCALF

Understanding Carbon-14 production in UK Magnox reactors by activation modelling and mass balance studies

Martin Metcalf, Senior Fellow in Graphite Technology at National Nuclear Laboratory.
Building 102 (B), Stonehouse Business Park, Bristol Road, Stonehouse, Gloucestershire, GL10 3UT

^{14}C measurements on core graphite, complementary experimental work, activation modelling and an assessment of reactor discharge histories have been used to improve understanding of the major pathways for the formation and loss of ^{14}C over the life of a Magnox reactor.

ERNASTAS NARKUNAS

Modelling of C-14 production in irradiated graphite of RBMK–1500 reactors and comparison with experimental data

In Lithuania, two RBMK-1500 water-cooled graphite-moderated channel-type power reactors at Ignalina Nuclear Power Plant (INPP) are under decommissioning now. The total mass of irradiated graphite in the cores of both units is more than 3600 tons. One of the main sources of uncertainty in the numerical assessment of radionuclides activity in the graphite is the uncertainty of the initial impurities content in it. Nitrogen is one of the most important impurities, having a large neutron capture cross-section, and thus may become dominant source of C-14 production. RBMK reactors graphite stacks operate in the cooling mixture of helium-nitrogen gases and this may additionally increase the quantity of nitrogen impurity. In this presentation the results of numerical modelling of graphite activation for the INPP Unit 1 reactor are presented. In order to evaluate the C-14 activity dependence on the nitrogen impurity content, several cases with different nitrogen content were developed taking into account initial nitrogen impurity quantities in the graphite matrix and possible nitrogen quantities entrapped in the graphite pores from the cooling gases. Additionally, comparison of the modelled C-14 activities with experimentally measured is also provided.

Radionuclide inventory determination of UK irradiated graphite wastes

G. Black1*, Dr L. McDermott1, Dr A. Jones1, Prof. B. Marsden1, C. Fisher2

1Nuclear Graphite Research Group, University of Manchester;

2 Office for Nuclear Regulation

*greg.black@postgrad.manchester.ac.uk

At present no long term decommissioning or final disposal options have been developed for nuclear graphite waste, it is the aim of this study to assist the UK regulatory authorities in the development of suitable programmes. The determining factor for safe disposal includes the final radionuclide inventory of the irradiated graphite; ^{14}C represents a significant proportion of this inventory. ^{14}C in graphite wastes may originate from direct neutron activation of the natural ^{13}C and ^{14}N impurity in the material at start of life or from coolant bound contamination transferred in the reactor circuit. This research will draw comparisons for both MTR and commercial reactor graphite to investigate the origin of ^{14}C, using reactor physics and activation codes in conjunction with experimental characterisation of irradiated graphite samples. Simulation research has involved modelling the neutron flux in each reactor using codes WIMS and MCBEND, followed by the neutron-activation calculation using the code FISPACT.

3.3 Ways forward

It was highlighted that within the UK there were good links between groups working on atomistic modelling of graphite, members from this area were keen to collaborate with the work being undertaken by Jean-Marc Leyssale as detailed in the presentation: *'Nanostructure of Pyrocarbon Matrices: from experimental characterizations to atomistic models'*. It was also highlighted that this work could be linked with the experimental capabilities discussed in the presentations '*In-situ transmission electron microscopy studies of ion-beam induced radiation damage in graphite'* and *'The Use of Small Angle Neutron*

Scattering in the Study of Porosity in Nuclear Graphite'. Collaboration between S.E. Donnelly and Lyon in in the field of insitu ion irradiation experiments is underway.

4 Summary

This task has built on analysis of data for the various grades of unirradiated and irradiated graphite obtained in WP3 in conjunction with data obtained for treated graphite in WP4. Mechanistic background of impurity / isotope localisation before and after treatment is required to feed into the treatment options within WP4 and subsequent work packages. The process involved in predicting the end of life radionuclide inventory has been identified and research is underway in order to apply this to a statistical model for impurity removal in WP4. Techniques such as Autoradiography and X-ray tomography have been highlighted for the analysis of impurity and isotopic location within the irradiated graphite material. A meeting held in Manchester brought together experts in the fields of atomistic, experimental analysis and neutronics/activation modelling to discuss future collaboration in the development of a fuller understanding of the behaviour of 14C formation and location. A fundamental understanding of radionuclide origins, location as removal mechanisms, combined with the development of improved graphite purification methods, may enable the manufacture of new grades of nuclear graphite with lower impurity concentrations being important for both improved neutronics and waste minimisation.

5 References

1. Nightingale, R.E., *Nuclear Graphite*. 1962, New York: Academic Press.
2. Wickham, A.J. and B.J. Marsden, *Characterisation, Treatment and Conditioning of Radioactive Graphite from Decommissioning of Nuclear Reactors.* IAEA TECDOC-1521,, 2006.

3. White, I.F., et al., *Assessment of Graphite management modesfor graphite form reactor decommissioning*, in *CEC*, E. Commission, Editor 1984.
4. Fachinger, J., *14C and 3H Thermal Treatment from Merlin Graphite*, in *CARBOWASTE: 2nd Annual steering committee meeting*, A.N. Jones, Editor 2009: Marcoule, France.
5. FZJ, *CARBOWASTE Treatment and Disposal of Irradiated Graphite and Other Carbonaceous Waste Grant agreement no.: 211333*, 2008.
6. von Lensa, W., *CARBOWASTE: New EURATOM Project on 'Treatment and Disposal of Irradiated Graphite and other Carbonaceous Waste'*, in *Proceedings of the 4th International Topical Meeting on High-Temperature Reactor Technology*, HTR2008, Editor 2008: Washington D.C., USA.
7. Guiroy, J.J., *Graphite waste incineration in a fluidized bed*, in *Specialists meeting on graphite moderator lifecycle behaviour*, I.A.E. Agency, Editor 1995, International Atomic Energy Agency: Bath, UK. p. 193-203.
8. Kelly, B.T., *Graphite - The Most Fascinating Nuclear Material.* Carbon, 1982. 20(1): p. 3-11.
9. Hou, X., *Rapid analysis of 14C and 3H in graphite and concrete for decommissioning of nuclear reactor.* Applied Radiation and Isotopes, 2005. 62(6): p. 871-882.
10. Wampler, W.R., et al., *Trapping of deuterium at damage in graphite.* Journal of Nuclear Materials, 1990. 176-77: p. 983-986.
11. Hou, X., L.F. Ostergaard, and S.P. Nielsen, *Determination of 36Cl in Nuclear Waste from Reactor Decommissioning.* Anal. Chem., 2007. 79(8): p. 3126-3134.
12. Bauer, E., *STUDIES OF THE INITIAL PHASES OF OXIDATION OF NUCLEAR GRAPHITE IN AIR AT TEMPERATURES BETWEEN 420 AND 650 C.* Journal de Chimie Physique (France) Merged with Rev. Gen. Colloides to form J. Chim. Phys. Rev. Gen. Colloides; Vol: 58, 1961: p. Pages: 47-52.
13. *Introduction to Autoradiography.* 1998.
14. Berre, C., et al., *Numerical modelling of the effects of porosity changes on the mechanical properties of nuclear graphite.* Journal of Nuclear Materials, 2006. 352(1-3): p. 1-5.
15. Babout, L., et al., *The effect of thermal oxidation on polycrystalline graphite studied by X-ray tomography.* Carbon, 2005. 43(4): p. 765-774.
16. Babout, L., et al., *Three-dimensional characterization and thermal property modelling of thermally oxidized nuclear graphite.* Acta Materialia, 2008. 56(16): p. 4242-4254.

Appendix 1

Irradiation damage and ^{14}C formation in Nuclear Graphite Joint meeting in conjunction with the FP7 Carbowaste program

Staff House Room 8, 2nd floor, Conference Suite, Sackville street campus, the University of Manchester
28th Nov 2012

House keeping

- Automated Fire alarm – planned Wednesday afternoon from 3 – 3.30pm
- Any others alarms please leave the building out of the main entrance
- Wifi – via Eduroam
- Breaks - Common Room
- Lunch - Mumford Restaurant (downstairs)

Graphite moderated reactors: Past, present and future

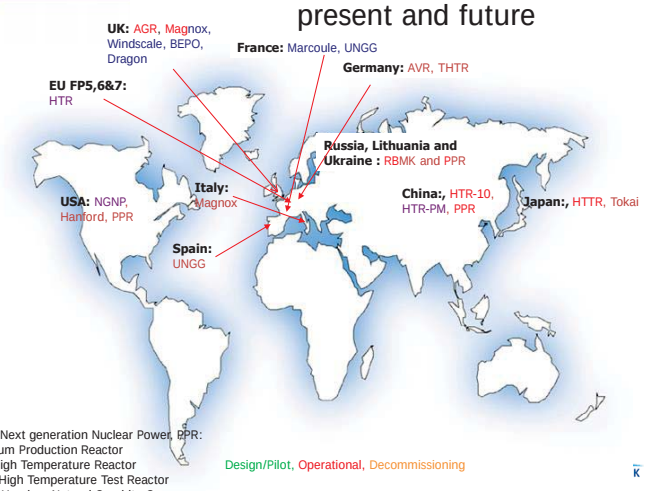

NGNP: Next generation Nuclear Power, PPR: Plutonium Production Reactor
HTR: High Temperature Reactor
HTTR: High Temperature Test Reactor
UNGG: Uranium Naturel Graphite Gaz

Graphite moderated reactor research:

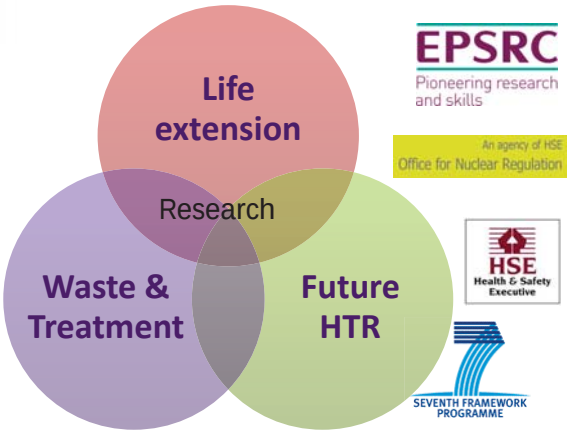

CARBOWASTE

'Treatment and Disposal of Irradiated Graphite and other Carbonaceous Waste'

- 6M€ EURATOM Framework 7 Project
- Consortium of 30 European partners (6 from UK)
- UoM work focuses on:-
  - WP3 Characterisations
  - WP4 Treatment
  - WP6 Long term behaviour

Work Package 1
- Identify magnitude of problem and major options from toolbox

Work Package 2
- Retrieval of i-graphite and interim storage considerations

Work Package 3
- Characterise structure, properties and contamination of i-graphite

Work Package 4
- Select i-graphite treatment options and determine decontamination factors

Work Package 5
- Re-use/ recycle and manufacture of new products

Work Package 6
- Determine long term disposal behaviour and waste packages/ conditioning

Disposal Options for irradiated graphite

- **Characterise**
  - Location of radioisotopes within the microstructure
- **Reduce isotopic content**
  - Pre-treatment of materials prior to disposal
- **Remove**
  - Direct chemical and physical thermal treatment using controlled chemical processes
- **Contain /disposal**
  - Requires an understanding of the final waste form behaviour under repository conditions

Capability and Future research

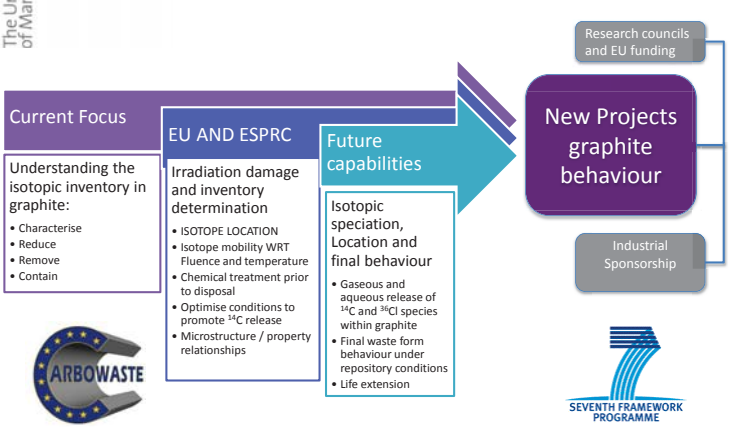

Agenda

8.30	Arrival - Tea & coffee available in the 2nd floor common room	
9.15	Welcome and introduction	Abbie Jones / Barry Marsden The University of Manchester
9.30	Carbowaste project and 14C Formation	Werner von Vensa Carbowaste co-ordinator, FZJ
10.00	Displacement damage in graphite – guidance from first principles and from the literature	Malcolm Heggie, University of Surrey
10.30	Nanostructure of Pyrocarbon Matrices: from experimental characterizations to atomistic models	Jean-Marc Leyssale CNRS, France
11.00	Coffee Break	
11.20	In situ ion irradiation of graphite	Steve Donnelly, University of Huddersfield
11.50	Synergistic or decoupled effects of temperature and irradiation on ^{14}C and ^{36}Cl behavior in irradiated graphite studied through ion implantation or irradiation of virgin nuclear graphite	Nelly Toulhoat, Université de Lyon
12.20	The Use of Small Angle Neutron Scattering in the Study of Porosity in Nuclear Graphite:	Keith Ross University of Salford
12.50	Discussions	
1.00	Lunch	
2.00	Irradiation Damage of Graphite in-reactor and its Disposal	John Lillington AMEC
2.30	Understanding Carbon-14 production in UK Magnox reactors by activation modelling and mass balance studies	Martin Metcalf NNL
3.00	Modelling of C-14 production in irradiated graphite of RBMK-1500 reactors and comparison with experimental data	Ernastas Narkunas LEI, Lithuania
3.30	Radionuclide inventory determination for UK irradiated graphite wastes	Greg Black The University of Manchester
4.00	Tea /Coffee break	
4.15	Ways forward open discussion	
5.00	Close of meeting	

ANY QUESTIONS?

Evening meal

- EastZEast
- Meet outside MCC 6.50pm
- Meal - 7pm

Introduction to the CARBOWASTE Project

'Treatment and Disposal of Irradiated Graphite and other Carbonaceous Waste'

Werner von Lensa
Forschungszentrum Juelich GmbH, Germany

Co-authors:

D. Bradbury, Bradtec Decon Technologies;
G. Pina, CIEMAT; M.J. Grave, Doosan Babcock Energy;
D. Vulpius, FZJ; A.W. Banford, NNL; B. Grambow, Subatech

Facts & Partners

- **Start:** **April 2008** (4.6 years now)
- **Duration:** **60 Months**
- **Total Budget:** **~ 11 Mio. EURO**
- **EU-Funding:** **6 Mio. EUR**

29 (31) Partners, 10 EU Countries & RSA

- **nuclear industries** (AMEC NNC, AREVA NP, Doosan Babcock, PBMR)
- **waste management companies** (Bradtec, Studsvik, Hyder, FNAG)
- **utilities** (EDF, Sogin, (EPRI))
- **graphite manufacturers** (GrafTech, SGL-Carbon)
- **waste management authorities** (ANDRA, NDA, ENRESA)
- **research** (CEA, CIEMAT, ENEA, FI, FZJ, INR, JRC, LEI, UK NNL, NRG, SCK•CEN, NECSA)
- **universities** (EMN, CNRS-ENS, IPNL, The University of Manchester)

Co-sponsors (ANDRA, EDF, HSE, NDA, etc.)

Objectives

- **Integrated waste management approach on**
  - **irradiated graphite (i-graphite) &**
  - **other carbonaceous waste (e.g. backed carbon, pyrocarbon)**
- **Development of 'Best Practices' in**
  - **Retrieval of i-graphite from reactor core,**
  - **Characterization of i-graphite features incl. origin of contamination,**
  - **Treatment / purification options,**
  - **Re-use / Recycling of i-graphite for different purposes,**
  - **Storage and Disposal behaviour**
- **‚Toolbox' for economical, environmental & sustainable options for**
  - **Legacy waste of reactors facing decommissioning**
  - **Management of i-graphite from future V/HTR, MSR & Fusionreactors**

Dimension of the Problem

- **About 250 000 tons already accumulated, worldwide**
- **Origin from different reactor types & retrieval options**
  - MAGNOX, UNGG, AGR, HTR
  - RBMK, MTR
  - Individual irradiation ‚history' and contamination sources
- **Various graphite grades and impurities**
- **Varying content of long-lived radioisitopes**
  - **^{14}C** plus **^{3}H, ^{36}Cl**, **^{60}Co**, ^{79}Se, ^{99}Tc, ^{129}I, ^{135}Cs, $^{152/154}$Eu etc.
- **Diverging national classifications (ILW, LLW, LLLW)**
- **Different i-graphite management strategies**

Impact of the i-Graphite ‚History' ?

- **Main features of i-graphite may already be ‚manufactured' into the material during the production process:**
  - Impurities are origin of neutron activation processes
  - Locations of impurities may determine location of activation products
- **Construction, Operation, Retrieval & Storage History ?**

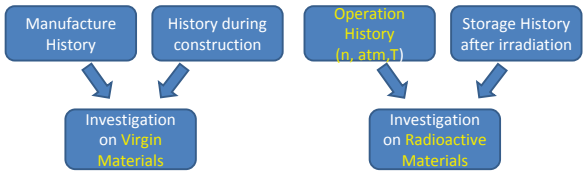

Location and Chemical Form of Activation Products ?

- Chemisorbtion of gases on surface of pore system (e.g. H_2, O_2, N_2)
  - Significant concentrations of nitrogen found by PGNA and in coolants
- ***Hypothesis***:
  - *^{14}C from nitrogen near to pore system surface & interface to coolant*
  - *^{14}C from ^{13}C as interstitial in the graphite lattice (diffusion?)*
  - ***At least two different locations / chemical bonds***
- Similar observations for other radionuclides
  - Organic **chlorine** in the bulk, inorganic forms at the inner surfaces
  - **Tritium** as H-T, C-T, C-OT, hydrocarbons (isotope exchange !)
  - **Metals** as carbides or ionic bonds

Impact of Activation Process ?

- Relevant activation processes show significant **recoil energies**

Nuclide	Max. released Energy (MeV)	Recoil Energy of Activation Product (keV)	Nucl. Reaction
H-3	6,25	7,0	6Li(n,α) H3
C-14	0,58 (p)	41,4	14N(n,p)C14
C-14	8,17	2,60	13C(n,γ)C14
O-17	2,42	0,19	17O(n,α)C14
Cl-36	7,80	0,91	35Cl (n,γ) Cl36
Co-60	6,70	0,40	59Co(n,γ)Co60

- Recoil energy **breaking pre-existing chemical bonds**
- Activation product is more or less **delocated**
- Ionizised activation product can form **new chemical bonds**

Radiocarbon in disordered structure

Impact on Treatment and Disposal ?

- **Exposed locations** of radionuclides at (pore) surfaces ?
- **Stable locations** within the crystallites ?
- **Migration** of interstitials to grain boundaries influenced by radiation damage ?
- **Labile and stable** chemical forms ?
- *Hypothesis:*
  - *Exposed and labile fractions may be removed by treatment and/or leaching*
  - *Stable fractions may withstand long-term leach attack*

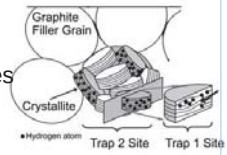

H. Atsumi, T. Tanabe, T. Shikama, Hydrogen Behavior in Carbon and Graphite before and after Neutron Irradiation -Trapping, Diffusion and the Simulation of Bulk Retention-, Journal of Nuclear Materials (2010), doi: 10.1016 / j.jnucmat.2010.12.100

Scope for the Joint Meeting

- Bring waste management & structural i-graphite science together
- **Better understand atomistic irradiation-induced processes**
  - Location of activation products ?
  - Chemical speciation of activation products ?
  - Temperature-induced migration of activation products ?
  - Agglomeration of activation products at pore surfaces / grain boundaries ?
  - Impact of radiolytical corrosion on release of activation products ?
  - Structural change of i-graphite by irradiation ? … ???
- **Symbiosis from operational & waste management knowledge**

Thanks for Your Attention !

+49 175 1876566 (mobile)

+49 2461 61 6629 (office)

w.von.lensa@fz-juelich.de

Homepage
www.carbowaste.eu

Registration: www.sinter.eu

INBK
INSTITUT FÜR NUKLEAREN BRENNSTOFFKREISLAUF

RWTH AACHEN UNIVERSITY

Molecular dynamic simulation of the transport behavior of C-14 in irradiated nuclear graphite

R. Nabbi, H. Probst

Motivations

- High amount of irradiated and radioactive nuclear graphite
- Need to dispose of by separation of radionuclides (H-3, C-14, …)
- Problem with C-14: similar chemical behavior as C-12
- To understand transport, bonding and configuration of C-14

INBK RWTH AACHEN UNIVERSITY

Contribution to the CARBOWASTE Project

++ Single effect analysis
=> 14C-Formation: Activation and irradiation
=> Formation of point defects and Frenkel pairs
=> damage rate

++ The kinetics of the recoil atoms
=> interaction and cascade process
=> damage concentration and configurations

++ Mechanisms of 14C-transport
=> in pure graphite (crystaline structure)
=> The effect of grain boundaries, pores and inhomogeneities

++ Effect of impurities and atomic additives (N, O, H, …)
(preferential accumulation and bonding, 14C)

INBK RWTH AACHEN UNIVERSITY

Source and Production

- Directly by:
  - $^{14}N(n,p)^{14}C$, $\sigma_{th} = 1.827\ barn$
  - $^{13}C(n,\gamma)^{14}C$, $\sigma_{th} = 1.37\ mbarn$
  - $^{17}O(n,\alpha)^{14}C$, $\sigma_{th} = 235\ mbarn$

  (N and O in pores (on inner surfaces), in cooling, cover gas)
- Indirectly: ,

$$^{12}C(n,\gamma)^{13}C \qquad ^{16}O(n,\gamma)^{17}O$$

INBK RWTH AACHEN UNIVERSITY

Neutron spectrum und cross section for different nucl interactions

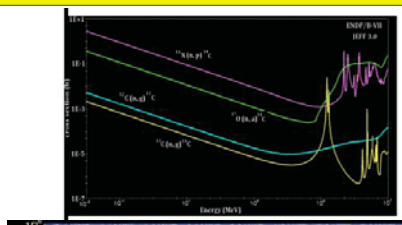

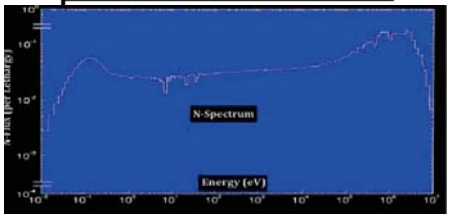

INBK RWTH AACHEN UNIVERSITY

Mechanism of single atom displacement

(Neutron absorption, gamma-emission, 14C displacement)

$E_r = 5.4 \times 10^{-4} \quad E_\gamma^2 / A$

(The conservation of momentum implies that the emi

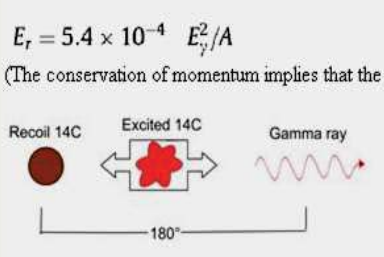

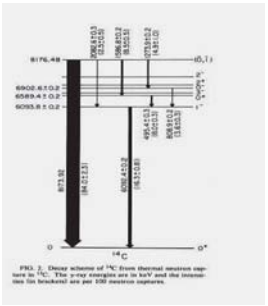

INBK RWTH AACHEN UNIVERSITY

Transport and Stopping

Typical recoil energies:

- by C-13: 2.56 keV
- by N-14: 42 keV

➡ cascades with ranges < 100 nm and < 250 dpa

Much less than for energies transferred by fast neutrons

Nuclear and electronic stopping, chemical bonding

Simulation: Molecular Dynamics with LAMMPS

http://lammps.sandia.gov

Intermolecular Two body potentials

- Hardsphere-Potential: $U_{HS}(r_{ij}) = \begin{cases} \infty & \forall\ r_{ij} \le d \\ 0 & \forall\ r_{ij} > d \end{cases}$

  Kraft: DIRAC-Funktion
- Softsphere-Potential: $U_{SS}(r_{ij}) = \epsilon \left(\frac{\sigma}{r_{ij}}\right)^n$
- Square-well-Potential: $U_{SW}(r_{ij}) = \begin{cases} \infty & \forall\ r_{ij} \le d_1 \\ -\epsilon & \forall\ d_1 < r_{ij} < d_2 \\ 0 & \forall\ r_{ij} \ge d_2 \end{cases}$
- SUTHERLAND-Potential: $U_{Su}(r_{ij}) = \begin{cases} \infty & \forall\ r_{ij} \le d \\ \frac{-\epsilon}{r_{ij}^6} & \forall\ r_{ij} > d \end{cases}$
- LENNARD-JONES Potential
- VAN DER WAALS-Potential $U_W(r_{ij}) = -4\epsilon\sigma^6 \left(\frac{1}{r_{ij}}\right)^6$
- COULOMB-Potential: $U_C(r_{ij}) = \frac{1}{4\pi\epsilon_0}\frac{q_i q_j}{r_{ij}}$

1

Cascades in bulk graphite: Perfect lattice structure

(C-14 PKA for given energy and random direction)

Cascade in graphite with 1 keV, parallel to z
lines indicating the origin of atoms (bondings to neighbouring atoms),

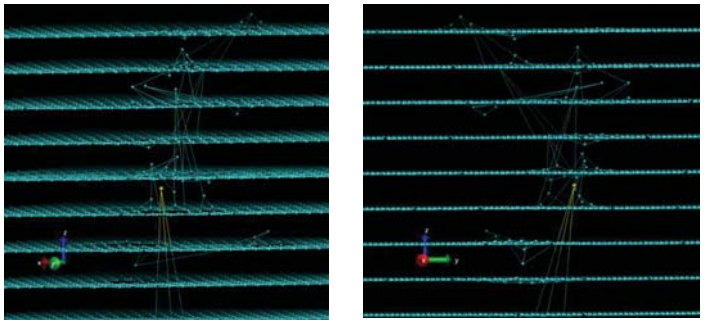

Cascades in bulk graphite:perfect lattice structure

(C-14 PKA for given energy and random direction)

Cascade in graphite with 1 keV, parallel to z, new bondings (configurations) at final state

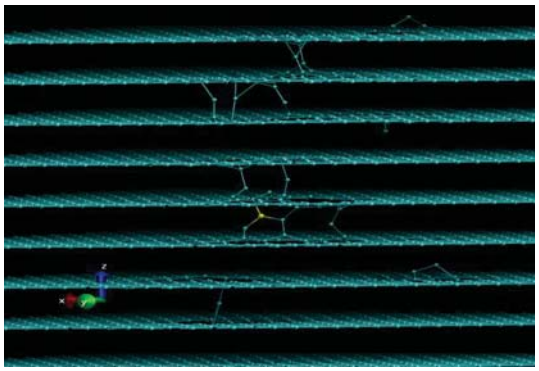

Perfect lattice structure: Displacement and energy loss

Exemplary run with 42 keV (left) and 100 keV (right)) (LCBOP)

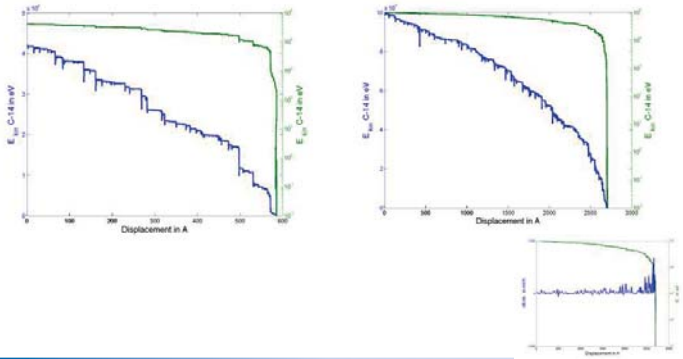

Cascades in bulk graphite

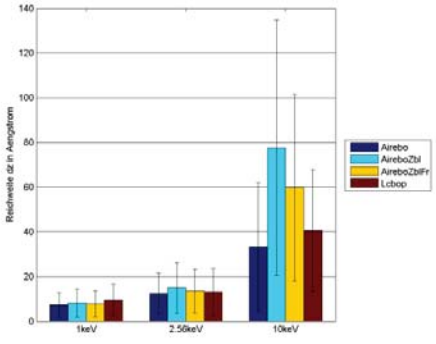

Range of PKA in Å in z-direction (parallel c);
random recoil direction,
temperature 300 K,
no significiant temperature dependence between 300 and 600 K (c.f. below)

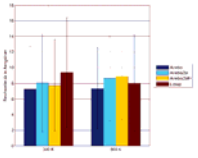

Cascades on grain boundaries

- Generated grain boundaries by two random oriented crystallites
- Find minimal energy state by displacement in x,y,z

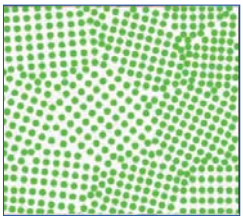

Crystallites configurations: Cascades on grain boundaries

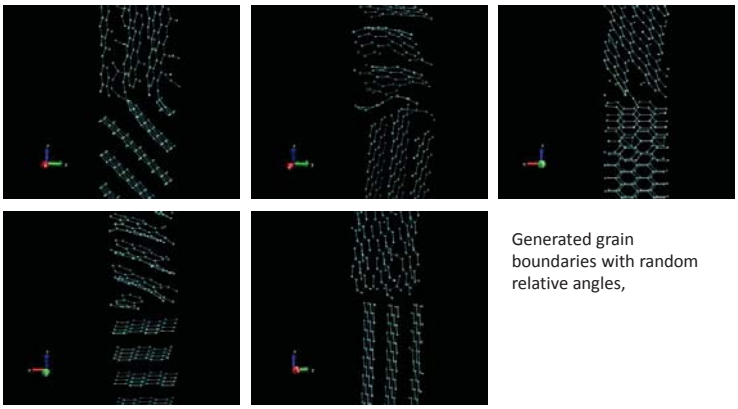

Generated grain boundaries with random relative angles,

Crystallites configurations: Cascades on grain boundaries

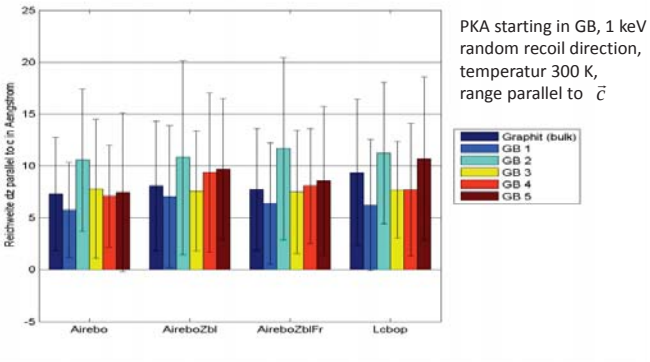

PKA starting in GB, 1 keV random recoil direction, temperatur 300 K, range parallel to $\vec{c}$

Crystallites configurations: Cascades on grain boundaries

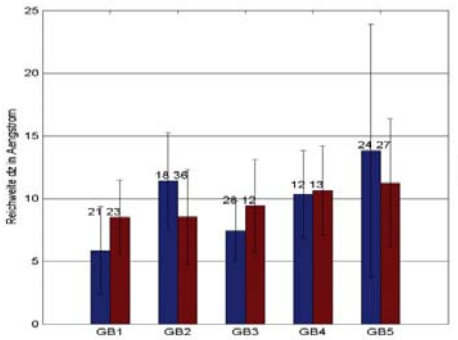

PKA starting ca. 6.7 above GB, energy 300 eV, temperature 300 K, random direction between 0-30° towards GB (blue) and in opposite direction (red);

Range |dz| in Å, additionally number of C14 rest in GB respective in comparable thick layer in other direction, potential LCBOP

Crystallites configurations: Cascades on grain boundaries

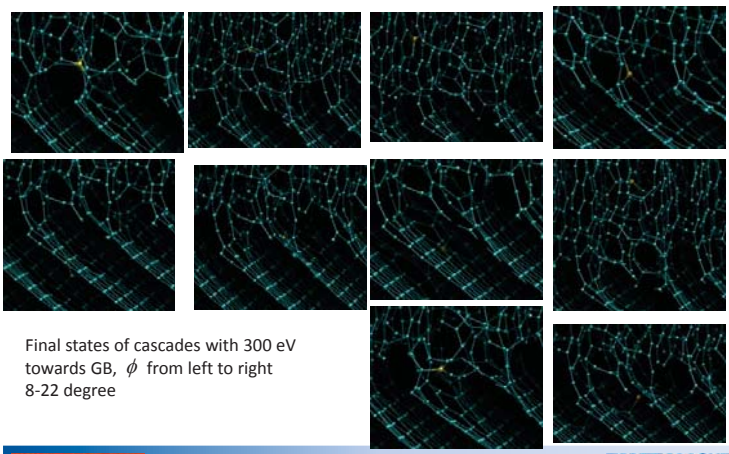

Final states of cascades with 300 eV towards GB, ϕ from left to right 8-22 degree

Effect of additive atoms and Interaction of 14C

- Let N and O be adsorbed on graphite surface
- various arrangments of adatoms
- Find minimal energy configuration (with ReaxFF)
- Here: two different concentrations of N and O

Effect of additive atoms and Interaction of 14C

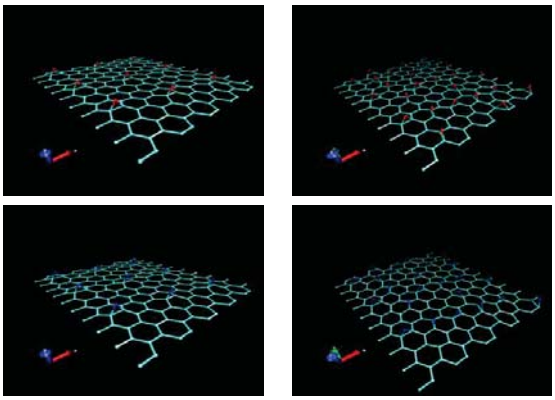

Equilibrium state by ReaxFF (energy minimization, local); red: O, blue: N, cyan: graphite lattice

Effect of additive atoms and Interaction of 14C

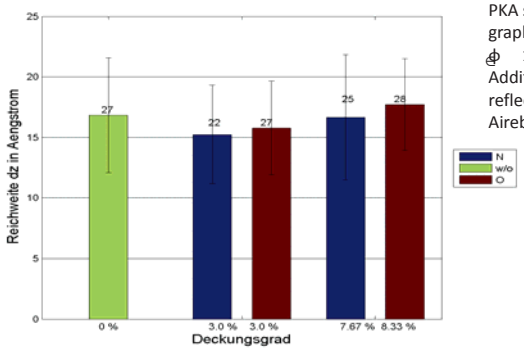

PKA started 9 Å above graphite surface, 1 keV
ϕ 120-180°,
Additional: number of non-reflected PKA (of 50 runs)
Airebo, LJ, Coul

Effect of additive atoms and Interaction of 14C

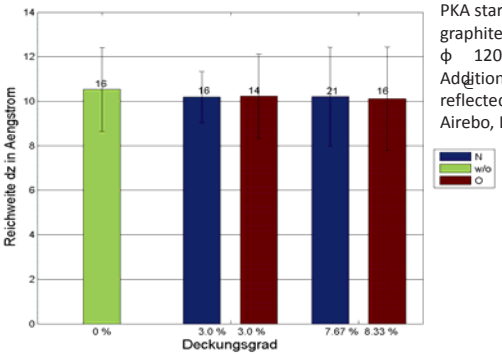

PKA started 9 Å above graphite surface, 200 eV
ϕ 120-180°,
Additional: number of non-reflected PKA (of 50 runs)
Airebo, LJ, Coul

Effect of additive atoms and Interaction of 14C

ReaxFF, 50 eV, 300 K, blau: N, gelb: C-14, cyan: C-12

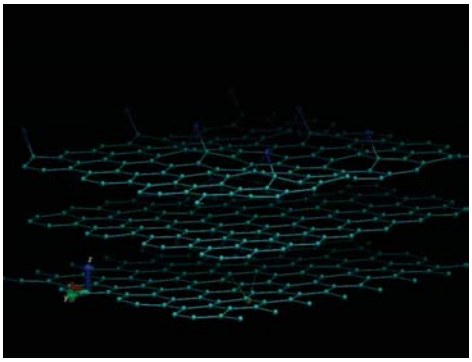

Effect of additive atoms and Interaction of 14C

ReaxFF, 50 eV, 300 K, blau: N, gelb: C-14, cyan: C-12

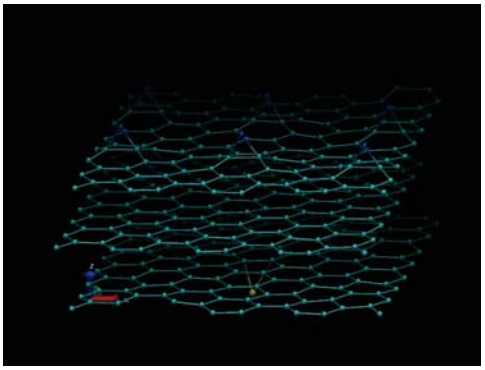

Cascades on surfaces with adsorbed atoms

ReaxFF, 50 eV, 300 K, blau: N, gelb: C-14, cyan: C-12

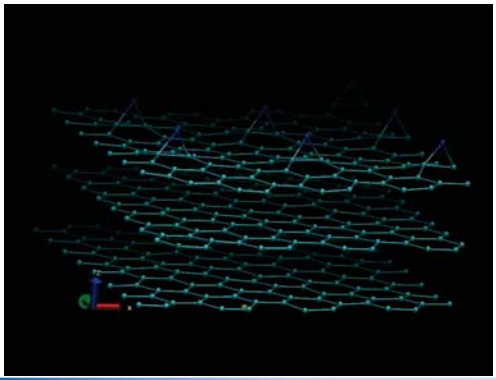


Thanks for your attention

Synergistic or decoupled effects of temperature and irradiation on ^{14}C and ^{36}Cl behavior in irradiated graphite studied through ion implantation or irradiation of virgin nuclear graphite

N. Toulhoat, N. Moncoffre, Y. Pipon, N. Bérerd
G. Silbermann PhD, A. Blondel PhD

Université Lyon 1, Institut de Physique Nucléaire de Lyon (IPNL), Villeurbanne

Context

- Dismantling of the UNGG (EDF&CEA)
  - Graphite moderated, fueled with natural uranium, CO_2 cooled
  - Dismantling planned latest by 2022

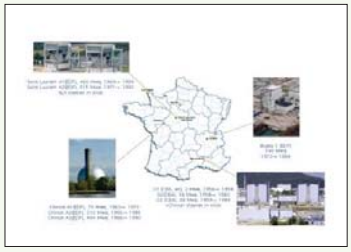

- 23 000 tons of graphite waste (UNGG + CEA + research reactors)
  - LL-LLW, underground disposal (down to 200 m) with an intact clay cover
  - Alternative management options are also foreseen (decontamination, deep disposal…)

[ANDRA]

Context

- 3 main radionuclides of concern for interim storage and disposal: ^{14}C, ^{36}Cl, ^{3}H
  - ^{14}C 5730 years : the main long lived radionuclide in terms of activity
  - ^{36}Cl 300 000 years : long lifetime and highly mobile in clay ⇨ determining for choosing graphite outlet
  - ^{3}H 12.3 years : mainly concerning during interim storage and disposal operation

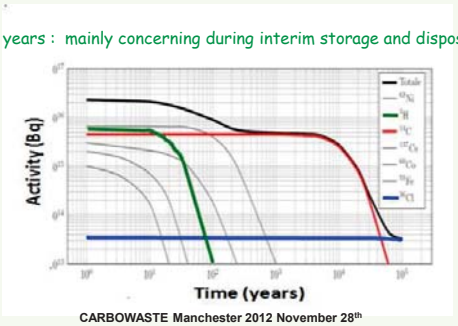

^{14}C and ^{36}Cl inventory

- EDF estimations on the French irradiated moderator graphite show that the ^{14}C and ^{36}Cl inventory does not match the initial precursor contents

⇐ part of ^{14}C and ^{36}Cl and even their precursors (nitrogen and chlorine) have been released during reactor operation

Our aim : help clarifying the ^{14}C and ^{36}Cl inventory

→ Obtain information on the bevaviour of ^{14}C and ^{36}Cl and their precursors during reactor operation

→ Obtain information on their distribution and speciation in the irradiated graphite

⇐ These data should be useful to optimise the purification solutions and disposal design

Method : Simulate the behaviour of ^{36}Cl and ^{14}C during reactor operation using stable isotopes

1. Implantation : Introduce a known quantity of ^{37}Cl and ^{13}C in graphite → To simulate ^{36}Cl and ^{14}C displaced from their original structural position through recoil during neutron irradiation

2. Study the independent effects and synergistic effects of

Temperature + **Irradiation** Neutron, gamma + **Radiolytic corrosion** gamma

Control ^{36}Cl and ^{14}C behaviour in reactor operating condition

Implantation, annealing, irradiation experiments

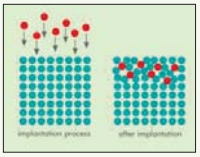

1 cm
1-2 mm

Polished graphite sample surface

SLA2 virgin moderator graphite

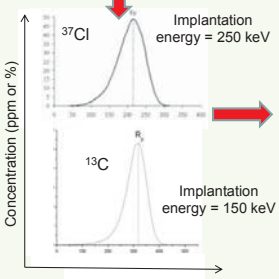

How do the profiles change with
Annealing
Irradiation
Radiolysis ?

Quantitative depth profile analysis and complementary characterisation

- Analysis of the implanted profiles : SIMS or RBS before and after treatment

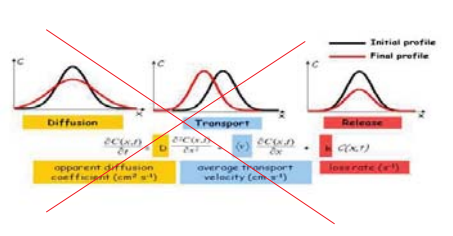

→ Main process : release

- - Checking of the structure by μRaman spectrometry (in collaboration with J.N. Rouzaud and M.R Ammar, ENS Paris)

- speciation determination by XPS or XAS, online or offline gas analysis (radiolysis experiments)

How do we simulate the effects of irradiation and temperature?

In reactor, radiation effects are mainly induced by

→ Neutrons (elastic collisions)

Atom displacements, vacancies (dpa)

simulated by low energy (≤1 MeV) heavy ion irradiation

→ Gamma radiation (inelastic interactions)

Graphite ionisation, gas radiolysis and corrosion at the gas/graphite interface

best simulated by :

-gamma irradiation (~ 1MeV) : $(dE/dx)_{elec} \approx 0.1$ keV/μm

enhanced by :

-alpha irradiation (~0.1 MeV to some MeV) : $(dE/dx)_{elec} \approx 100$ keV/μm

- heavy ion irradiation : medium (some tens of MeV) : or high energy (≥ 100 MeV) : $(dE/dx)_{elec} \approx$ up to 20 MeV/μm

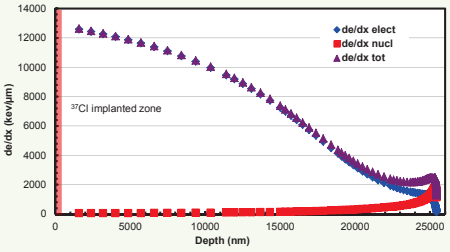

Evolution of the nuclear and electronic stopping power of 200 MeV Iodine ions in nuclear graphite

Annealing alone : secondary vacuum or inert gas

Furnaces

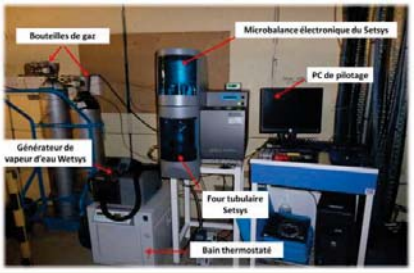

Thermogravimeter

Coupled Annealing/irradiation/radiolysis

Gamma radiation facility (ISOTRON) ^{60}Co gamma source : 1.17, 1.33 MeV (irradiation + radiolysis at RT)

4 MV Van de Graaff accelerator facility : ~7.5 MeV alpha beam (irradiation + radiolysis + annealing)

μGC-MS and irradiation cell

Orsay Tandem accelerator facility 200 MeV Iodine beam (irradiation + annealing)

Study on ^{13}C : used to simulate ^{14}C

$^{14}N(n_{th},p)^{14}C$	$^{13}C(n_{th},g)^{14}C$
s = **1,93** barn	s = **14x10^{-4}** barn
Predominant route if [N] > 8 at.ppm	Predominant route if [N] < 8 at.ppm
Graphite + contamination	Graphite

E=150 keV → Rp ~ 300 nm

f= 6x10^{16} at/cm² → $[^{13}C]_{RP}$ = 5 at.%

T=15°C and T=600°C

Two implantation temperatures :

15°C : very disordered structure

600°C : less disordered structure

→ Represent two different graphite ordering states in the reactor :

Disordered (high neutron flux, low temperature

Less disordered (low neutron flux, high temperature)

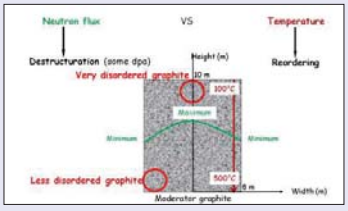

Cross section view

Raman + TEM characterisations (in collab. with J.N Rouzaud, M.R. Ammar)

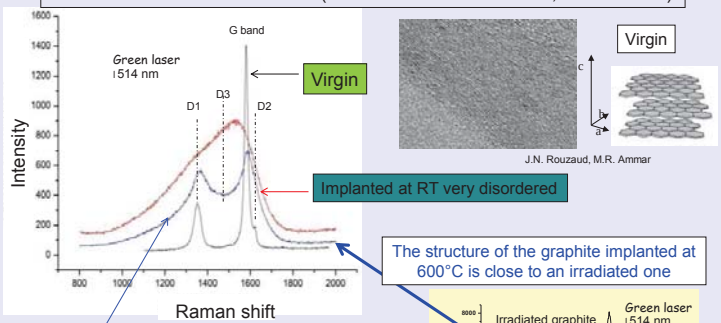

J.N. Rouzaud, M.R. Ammar

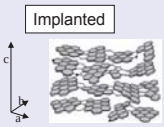

J.N. Rouzaud, M.R. Ammar

Implantation temperature effects on the release of ^{13}C

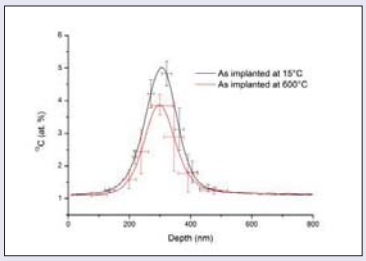

Implantation at RT

Rp = 301 ± 15 nm
FWHM = 127 ± 23 nm.
Area =1441 ± 36 at%.nm

Implantation at 600°C

Rp = 299 ± 35 nm
FWHM = 124 ± 58 nm.
Area = 1282 ± 27 at%.nm

→ The implantation at 600°C induces a release of ^{13}C around 11 ± 4 %

The released part corresponds probably to the ^{13}C located close to the open pores

↩ **During reactor operation, part of the ^{14}C might have been released as soon as produced in the hot parts of the reactor**

Temperature effects on the release of the implanted ^{13}C

^{13}C Implanted at RT (very disordered)

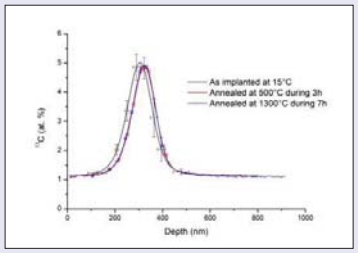

^{13}C Implanted at 600°C (less disordered)

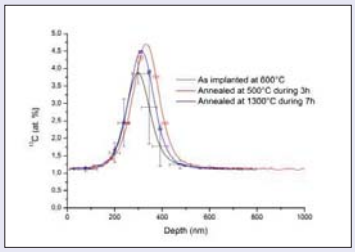

^{13}C is not released whatever the graphite disorder degree

Effect of coolant gas radiolysis and graphite irradiation on the release of ^{13}C

Initial coolant gas composition :
CO_2 mainly, CO 2,5 %, CH_4 500 ppm,
O_2 100 ppm H_2 100 ppm

µGC-MS coupled to the irradiation cell

Irradiation cell device modeled with MCNPX (Monte Carlo radiation transport code)

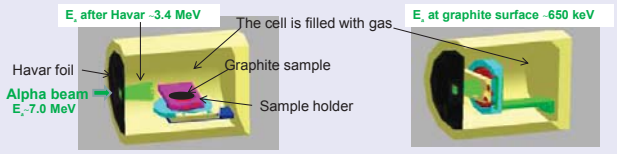

Alpha beam irradiates the gas only

Alpha beam irradiates gas + graphite

Gas irradiation / contact with a non irradiated heated graphite (500°C)

Two doses: 7 MGy and 15 MGy

Graphite implanted at RT

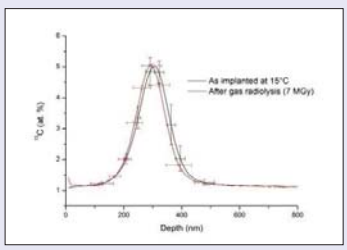

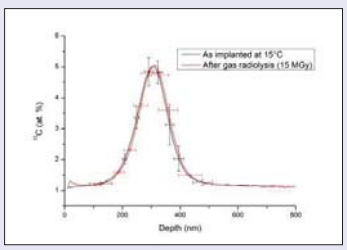

The ^{13}C profiles remain stable

The sample surface is not corroded (SEM)

→ Up to15 MGy, gas radiolysis does not seem to promote ^{13}C release in the graphite sample heated to 500°C

Gas irradiation / contact with an irradiated heated graphite (500°C), dE/dx_{elec} ~ 300 keV/µm : first results

Two doses: 5,8 MGy and 12,4 MGy

Irradiation fluence ~ 2 10^{15} ions.cm^{-2}
Flux ~ 2.9 10^{11} ions.cm^{-2}.s^{-1}

Graphite implanted at RT

Irradiation fluence ~ 4 10^{15} ions.cm^{-2}
Flux ~ 2.7 10^{11} ions.cm^{-2}.s^{-1}

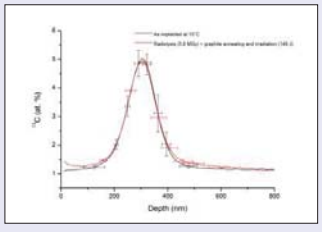

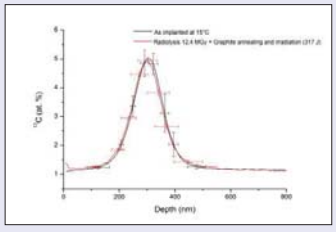

The ^{13}C profiles remain stable

The sample surface is not corroded (SEM)

→ Gas radiolysis and graphite irradiation do not seem to promote ^{13}C release in the graphite sample heated to 500°C (very first results, have to be checked)

Annealing, gas radiolysis and first graphite irradiation results show that ^{13}C is not released

Does ^{13}C migrate and form stable carbon clusters?

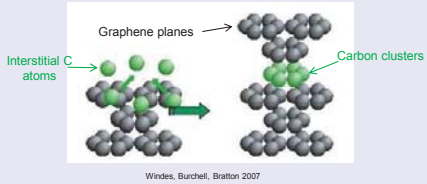

Windes, Burchell, Bratton 2007

Study on ^{37}Cl : used to simulate ^{36}Cl

$^{35}Cl(n_{th},g)^{36}Cl$

s = **33** barn

Predominant route

Graphite

E=250 keV → Rp ~ 220 nm

f≈ 5x10¹³at/cm² → $[^{37}C]_{RP}$ = 40 at.ppm

f≈ 2x10¹⁶at/cm² → $[^{37}C]_{RP}$ = 1at.%

T=15°C

Two different implantation fluences :

Low fluence : low [37Cl] , low disorder level (<< 1dpa)

High fluence : high [37Cl], higher disorder level (2-3 dpa)

Represent the heterogeneous chlorine concentration mapped by SIMS

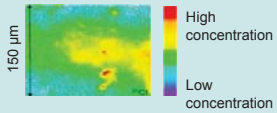

$1 < [Cl]_{pristine} < 15$ (at.ppm)

Temperature effects on the release of ^{37}Cl (in vacuum or argon)

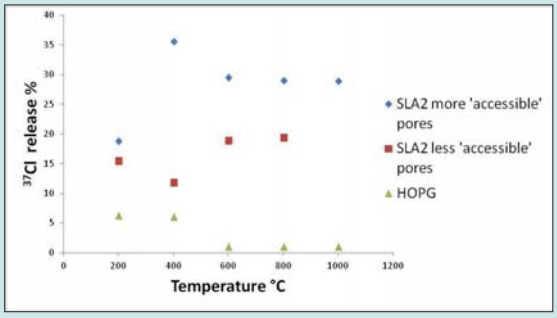

Maximum ^{37}Cl release around 30% for SLA2

Almost no release for HOPG

C.E. Vaudey PhD 2010

Pores are preferential release pathways for chlorine

Effect of **coolant gas radiolysis** on the release of ^{37}Cl

Alpha irradiation of gas + non irradiated heated graphite (500 °C)

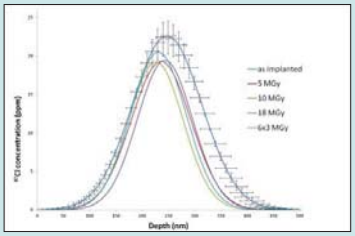

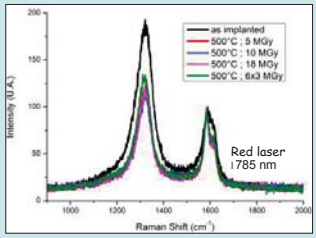

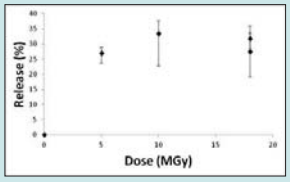

Radiolysis of coolant gas in contact with heated graphite implanted at $[^{37}Cl]Rp$ ~ 40 ppm seems to impact ^{37}Cl release : ~ 30 % (compared to 15% with temperature alone for the same kind of graphite)

Synergistic effect of graphite temperature + gas radiolysis on ^{37}Cl release

Effect of **coolant gas radiolysis and graphite irradiation** on the release of ^{37}Cl

Gamma irradiation of gas + graphite (not heated)

Gamma radiation facility (ISOTRON) (irradiation + radiolysis)

- ^{60}Co source (3 MCi ↔ ≈ 1.1 x 10^{11} Bq).
- Samples + coolant gas sealed vials.
- Room Temperature only
- Max Dose ~ 5 MGy

^{37}Cl concentration 40 ppm

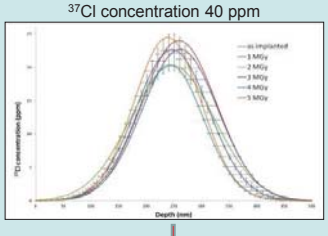

Gamma radiolysis $(dE/dx)_{elec}$ < 1 keV/µm + irradiation of a graphite implanted at $[^{37}Cl]Rp$ ~ 40 ppm does not impact ^{37}Cl release for doses up to 5 Mgy when the sample is not heated

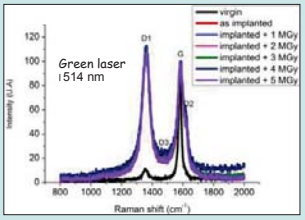

Effect of **graphite ~ 200 MeV iodine irradiation** (dE/dx_{elec} ~ 13 MeV/µm) on the release of ^{37}Cl (no coolant gas, vacuum irradiation)

^{37}Cl rich and disordered

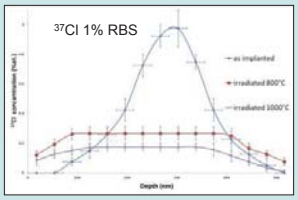

^{37}Cl rich and disordered

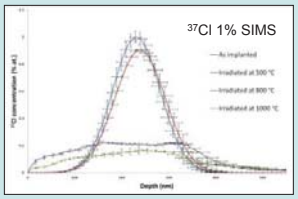

Irradiation fluence 500°C / 800°C / 1000°C ~ 3.4 10^{15} / 1.7 10^{15} / 2.0 10^{15} ions.cm^{-2}

Flux 500°C / 800°C / 1000°C ~ 1.8 10^{10} / 8.4 10^{10} / 8.6 10^{10} ions.cm^{-2}.s^{-1}

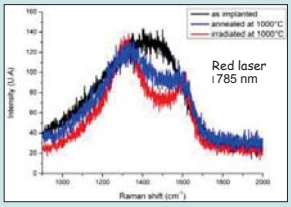

High dE/dx_{elec} + temperature induce a strong ^{37}Cl release and reorder the disordered graphite structure more than temperature alone does

Effect of **graphite ~ 200 MeV iodine irradiation** (dE/dx_{elec} ~ 13 MeV/µm) on the release of ^{37}Cl (no coolant gas, vacuum irradiation)

Low [^{37}Cl] less disordered

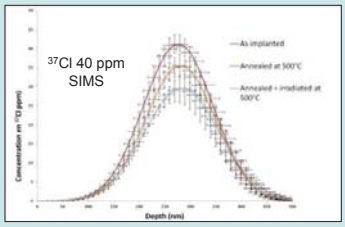

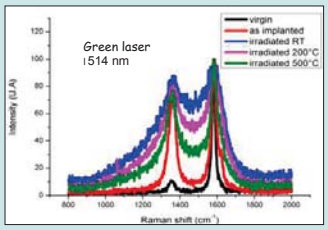

Irradiation fluence ~ 2.1 10^{15} ions.cm^{-2}
Flux ~ 1.0 10^{11} ions.cm^{-2}.s^{-1}

-Irradiation + annealing at 500°C seems to promote ^{37}Cl release

- Irradiation disorders whereas temperature orders the structure

Summary : Irradiation / Annealing

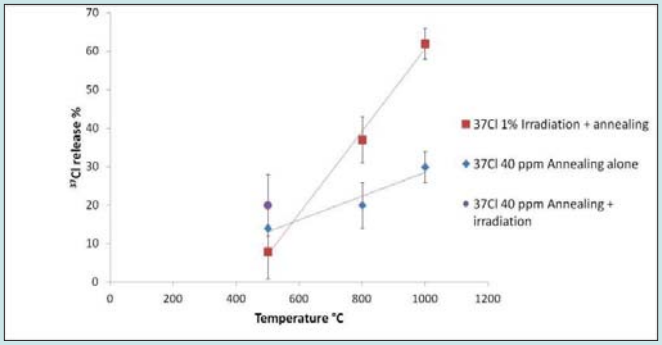

High dE/dx_{elec} + high temperature : promote ^{37}Cl release

of highly enriched and disordered zones

Conclusion

- Carbon and chlorine have very different behaviour
- ^{13}C is very stable whatever the structure (disordered or ordered) until 1300°C

  Gas radiolysis alone or coupled to graphite irradiation (at low dE/dx_{elec} ~ some 100keV/µm) does not promote its release on a heated (500°C) sample

→ In reactor graphite formation of stable ^{14}C - C clusters ?

- ^{13}C is released (~ 10%) during implantation at 600°C

→ In reactor part of the ^{14}C is probably released through the interconnected pores as soon as formed

- The irradiation (ionisation processes, higher dE/dx_{elec}) effects have to be checked

- ^{37}Cl is released with temperature (~ 15 to 30 % max after a few hours) at 500°C
- Radiolysis + temperature seem to promote slightly ^{37}Cl release even at 500°C
- ^{37}Cl is sensitive to ionising radiation and high dE/dx_{elec} promote its release especially at high temperatures and, to a lesser extent, at 500°C (i.e.reactor temperatures)

→ In reactor, temperature effects and ionisation processes might promote the ^{36}Cl release

- As for ^{14}C, in reactor part of the ^{36}Cl is probably released as soon as formed but this has to be checked
- ^{37}Cl behaviour must be tested during irradiation experiments at medium dE/dx_{elec}

BONUS SLIDES

Gamma radiolysis $(dE/dx)_{elec}$ < 1 keV/µm + irradiation of a graphite implanted at [^{37}Cl]Rp ~ 40 ppm does not impact the pore volumes for doses up to 5 Mgy when the sample is not heated. The speciation is mainly organic (C-Cl bonds)

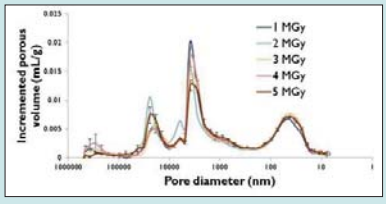

Pore volume

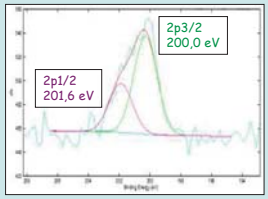

XPS spectrum

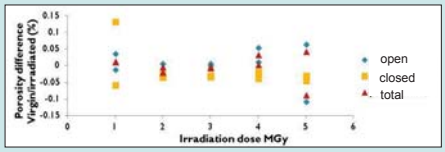

Gas irradiation / contact with an irradiated heated graphite (500°C)

The aim is to produce the maximum ionisation in the implanted zone (depth ~300 nm)

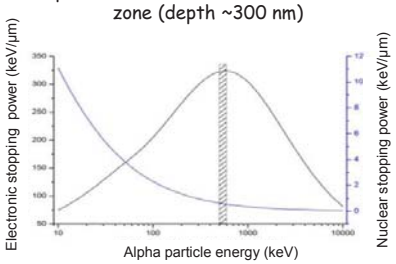

Alpha energy before the Havar foil : 6,95 MeV

Alpha energy after the Havar foil : 3, 38 MeV

Alpha energy at the graphite surface : 647 keV

THE USE OF SMALL ANGLE NEUTRON SCATTERING IN STUDY OF REACTOR GRAPHITE.

Dr. Zhanna Mileeva

The University of Salford

Introduction. Properties of neutrons.

- Interact with atomic nuclei rather than with the electronic cloud (the case with X-Rays), hence offering a direct probing of spatial distribution and structure.
- Allow to study the bulk of the materials without damaging them because of high penetration power of neutrons due to the relatively small neutron scattering cross sections of all elements.
- Ability to detect light atoms (including hydrogen) in the presence of heavy elements.
- Convenient neutron wavelengths span the atomic and macroscopic ranges (from several angstroms to a hundred of nanometers) which makes them perfect probes for material structure investigation.
- The unique property to distinguish isotopes of the same element due to a random variation of the strength of neutron-nucleus interaction with the atomic and mass numbers.

All these specific characteristics make neutron scattering a unique technique in studying porous amorphous structures in the mesoscopic range.
Moreover neutron scattering from a porous system delivers a direct measurement of a sample whereas other methods (e.g., gas sorption) imply some simplifying assumptions or (SEM, TEM, etc.) detect the surface but not the bulk properties.

Introduction. Principles of Small Angle Neutron Scattering.

The structure of the sample probed determines the neutron scattering, measured as a function of the scattering angle which is then converted into a measure in reciprocal space, the wave vector transfer, Q. The information about the structure of the sample can be obtained from an analysis of the measured distribution of scattering intensities over the range of Q.

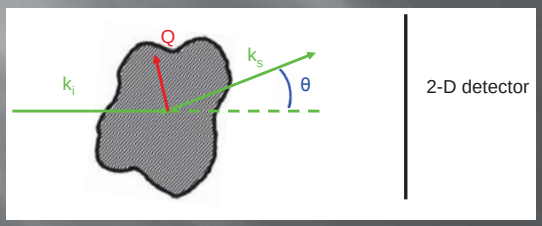

Scheme of neutron scattering.

Introduction. Principles of Small Angle Neutron Scattering.

For elastic scattering $|k_i| = |k_s| = 2\pi/\lambda$.

The wave vector transfer, Q, is a vector formed by subtraction of k_i from k_s and for elastic scattering is:

$$Q = \frac{4\pi}{\lambda}\sin\frac{\theta}{2}$$

Considering neutron diffraction and Bragg's Law we can obtain a relation between the wave vector transfer, Q, and the plane spacing, d:

$$Q = \frac{2\pi}{d}$$

This equation allows us to "size" the scattering particles (e.g., pores).

It can be clearly seen that smaller Qs respond to larger structures and vise versa.

Introduction. Principles of Small Angle Neutron Scattering.

The SANS intensity (or the number of neutrons of a given wavelength per unit time per unit solid angle) scattered by a sample into a detector at a wave vector transfer, Q is given by:

$$I(Q) = I_0(\lambda)\Delta\Omega\eta(\lambda)TV\frac{d\Sigma}{d\Omega}(Q)$$

$I_0(\lambda)$ is the incident neutron flux/unit wavelength

$\Delta\Omega$ is the solid angle of the detector element

$\eta(\lambda)$ is the detector efficiency

T is the sample transmission

V is the sample volume

$\boldsymbol{d\Sigma/d\Omega(Q)}$ is the differential scattering cross section – the Fourier Transform of the neutron scattering length density-density correlation function of the pores – is defined by the size, shape and arrangements of the scattering density fluctuation.

Introduction. Principles of Small Angle Neutron Scattering.

The differential scattering cross section can be written generally for a two-phase system and, particularly, for pores in carbon in terms of the neutron scattering length density of the carbon, δ_c and of the scattering density in the pore, δ_p:

$$\frac{d\Sigma}{d\Omega}(Q) = N_p V_p^{\,2}(\delta_c - \delta_p)^2 S(Q)P(Q) + B_{inc}$$

N_p is the number of pores per unit volume

V_p is the volume of the pore

$S(Q)$ is the structure factor for the separation of the pore centres

$P(Q)$ is the form factor for the pores (also denoted as $F^2(Q)$)

B_{inc} is the flat (Q-independent) background

The neutron scattering length density is the product of the neutron scattering length, b, and number of nuclei per unit volume:

$$\delta = \sum_i b_i \frac{DN_A}{M_W}$$

THE USE OF SMALL ANGLE NEUTRON SCATTERING IN STUDY OF REACTOR GRAPHITE.

Contrast Matching technique.

The Contrast Matching technique is based on a difference in neutron scattering lengths of various elements and their isotopes. I.e. by varying the isotope ratio within a substance one can alter the average scattering length of a material and thus its scattering length density.

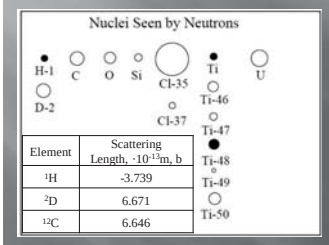

Element	Scattering Length, $\cdot 10^{-13}$m, b
^{1}H	-3.739
^{2}D	6.671
^{12}C	6.646

Neutron scattering lengths for several elements. Negative lengths are represented by dark circles.

$$\frac{d\Sigma}{d\Omega}(Q) = N_p V_p^{\,2} (\delta_c - \delta_p)^2 S(Q) P(Q) + B_{inc}$$

differential scattering cross-section

contrast term

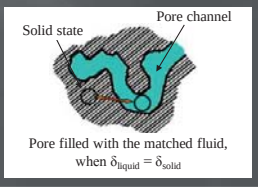

Pore filled with the matched fluid, when $\delta_{liquid} = \delta_{solid}$

THE USE OF SMALL ANGLE NEUTRON SCATTERING IN STUDY OF REACTOR GRAPHITE.

Fractals.

Fractals are defined as materials in which the geometric structure is independent of the length scale on which it is observed. This is strictly true for geometric fractals such as those investigated by Mandelbrot. More commonly in Nature the features are actually random, being only *self-similar* when viewed on different length scales.

Activated carbons, produced from a vegetable source which is typically fractal, retain the fractal geometry of the original material after pyrolysis.

It is also found in materials such as graphite that $d\Sigma/d\Omega(Q)$, and thus $S(Q)$, can be represented by a power law with a non-integer negative exponent and this indicates the presence of a pore fractal.

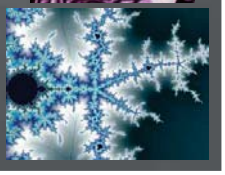

THE USE OF SMALL ANGLE NEUTRON SCATTERING IN STUDY OF REACTOR GRAPHITE.

Three classes of fractal.

Volume fractals – where the average density of a material decreases in a power law fashion as one moves out radially from an origin chosen to be in the solid phase. Such material is said to have a volume fractal dimension of D_m (< 3 in a 3-D space).

Pore fractals, where the distribution of pore volume decreases in a similar way with increasing distance from a pore centre. These would thus have a pore fractal dimension of D_p (< 3 in 3D).

Surface fractal – where the measured surface area increases in a power law fashion when measured using a decreasing tile size. Here the non-integer dimension is D_s where $2 < D_s < 3$.

THE USE OF SMALL ANGLE NEUTRON SCATTERING IN STUDY OF REACTOR GRAPHITE.

Identifying fractals

The main feature of fractals is a power law scaling of particular characteristic with probing length. Therefore, a fractal region can be identified when this relationship yields a straight line on log-log coordinates. Neutron scattering reveals the fractal nature of the sample when the scattering intensity (differential cross section) is plotted versus Q on a double logarithmic graph.

When, for these three types of fractal, the density-density correlations are converted to the differential scattering cross section form, the scattering will in general vary as:

$$S(Q) \sim Q^{\,Ds\,-2(Dm\,+\,Dp)\,+\,6}$$

For a surface fractal, we take $D_m = D_p = 3$ so that $I(Q) \sim Q^{Ds-6}$ as first derived by Bale and Schmidt. Here, in general, the scattering varies with powers of Q between -3 and -4.

For a volume fractal, we take $D_s = D_m$ and $D_p = 3$ so that S(Q) varies as Q^{-Dm} while for a pore fractal, we similarly get $S(Q) \sim Q^{-Dp}$.

For a smooth surface Euclidean dimension is 2, thus $I(Q) \sim Q^{2-6} = Q^{-4}$

THE USE OF SMALL ANGLE NEUTRON SCATTERING IN STUDY OF REACTOR GRAPHITE.

Fractal graphite structure.

Replotting of early SANS measurements (D.G. Martin and J. Caisley, Carbon, 1977. Vol. 15, pp. 251-255.) on a log-log scale have shown that for AGR (Gilso) graphites, the SANS has a non-integer power law intensity variation with wave vector transfer (Q) over three orders of magnitude and the non-integer index value extracted from these data varies with fast neutron irradiation.

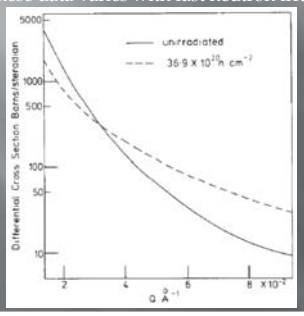

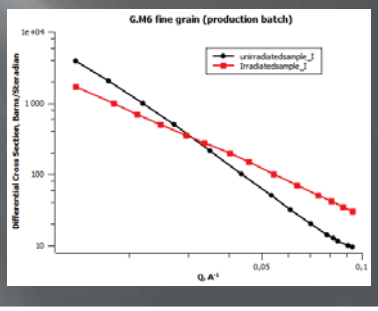

THE USE OF SMALL ANGLE NEUTRON SCATTERING IN STUDY OF REACTOR GRAPHITE.

Fractal graphite structure.

The scattering from unirradiated sample (G.M6) falls clearly into two distinct linear regions with gradients -2.86 at low Q (volume fractal) and -3.46 at higher Q (surface fractal).

Data from irradiated samples have remarkably changed to give a good linear behavior for the full Q range measured with a gradient of -2.075, a volume/mass fractal. The scattering from the surface seems to have been suppressed. The obvious conclusion is that the irradiation process has reduced the surface area.

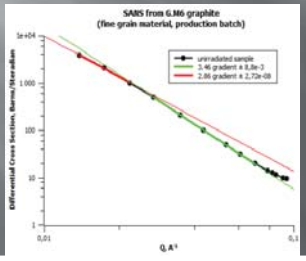

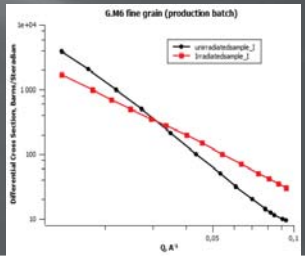

THE USE OF SMALL ANGLE NEUTRON SCATTERING IN STUDY OF REACTOR GRAPHITE.

Fractal graphite structure and its evolution with neutron irradiation.

For AGR (Gilso) graphites, the SANS has a non-integer power law intensity variation with wave vector transfer (Q) over three orders of magnitude and the non-integer index varies with irradiation (as shown for GE1). This suggests a fractal distribution of porosity which changes as the carbon atoms are displaced.

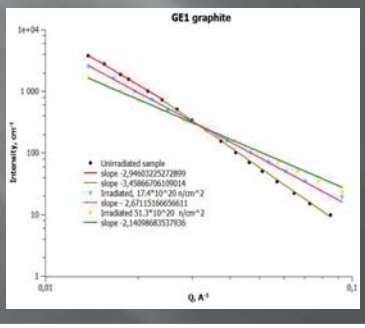

THE USE OF SMALL ANGLE NEUTRON SCATTERING IN STUDY OF REACTOR GRAPHITE.

Contribution of Mrozowski Cracks to the SANS from nuclear graphites.

Graphites might be expected to show several types of porosity including open pores created by decomposition gases, cracks between graphitic and amorphous carbon and internal cracks within the graphitized material which are produced as the graphitic particles cool below the plastic/solid transition, due to the anisotropic shrinkage along the c-direction (so-called Mrozowski cracks).

Re-analysis of existing SANS data on GILSO graphites suggests that the scattering from the graphitic coke particles shows a strong power law form. We have suggested that this fractal distribution of pore widths has to be due to the existence of Mrozowski cracks.

According to our hypothesis, these cracks – and hence the associated SANS - should disappear when the graphite is heated up to the plastic deformation temperature of the amorphous carbon matrix formed from the pitch binder.

THE USE OF SMALL ANGLE NEUTRON SCATTERING IN STUDY OF REACTOR GRAPHITE.

Contribution of Mrozowski Cracks to the SANS from nuclear graphites.

Our recent measurements of the variation of the SANS for PGA graphite as a function of temperature show that the intensity of the SANS decreases more or less linearly with temperature but with little change in the power law index.

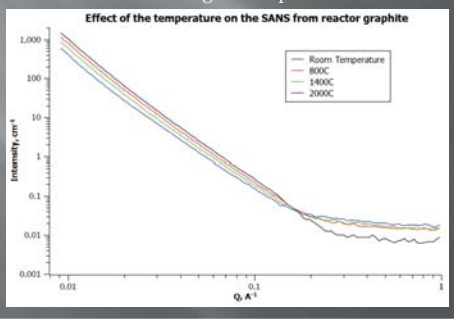

THE USE OF SMALL ANGLE NEUTRON SCATTERING IN STUDY OF REACTOR GRAPHITE.

Contribution of Mrozowski Cracks to the SANS from nuclear graphites.

It should be noted that the decrease is linear up to the maximum temperature measured which extrapolate to zero at about 3000°C, more typical of the maximum temperature reached in the graphitising of the coke grist than the processing temperature of the grist/binder mix. This, again, support our suggestion.

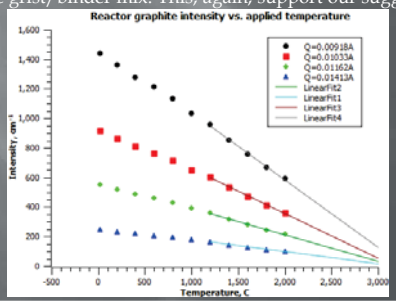

THE USE OF SMALL ANGLE NEUTRON SCATTERING IN STUDY OF REACTOR GRAPHITE.

Contribution of Mrozowski Cracks to the SANS from nuclear graphites.

Further contrast matching experiments on the same graphites show that the porosity can indeed be divided into open and closed pores. The remarkable result is that 60% of the porosity is open to the toluene adsorbate and that both components have a very similar SANS profile, and hence a similar distribution of pore sizes.

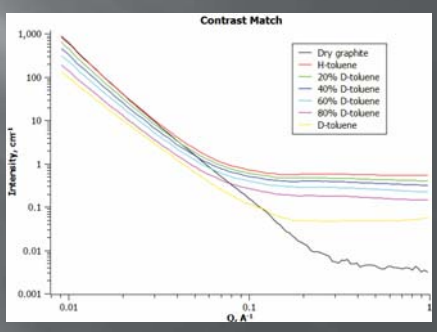

THE USE OF SMALL ANGLE NEUTRON SCATTERING IN STUDY OF REACTOR GRAPHITE.

SANS from reactor graphites. Conclusions.

Contrast Matching on reactor graphite allow us to distinguish open and closed porosity, giving a quantitative ratio between them.

A single power law form suggests a single origin for porosity that dominates the SANS. Our hypothesis is that this porosity is the result of Mrozowski Cracks – formed in the graphitic grist as it is cooled below the lowest plastic deformation temperature. These cracks form due to the anisotropic thermal expansion of the graphite.

As has been demonstrated in our recent SANS measurements the Mrozowski cracks are clearly also relevant to the radiolytic oxidation process in CO_2 cooled reactors. This follows from the observation that contrast matching experiments show that 60% of the power law scattering is removed by the addition of the contrast matching liquid.

Under combined fast neutron and gamma radiation in CO_2, the evolution of SANS is of considerable importance.


THE USE OF SMALL ANGLE NEUTRON SCATTERING IN STUDY OF REACTOR GRAPHITE.
Thank you for your attention.

Irradiation Damage and 14C Formation in Irradiated Graphite

Presentation to : Nuclear Graphite Research Group
Venue: University of Manchester
Presented by: Dr John Lillington
Date: 28th November, 2012

Sizewell-B (Courtesy of EDF Energy)

Summary

- Focus on AMEC's contribution on irradiation damage and ^{14}C formation in irradiated graphite associated with the following:
- Operational issues associated with the behaviour of graphite through life in the current reactor fleet
- Legacy waste management of graphite, other carbonaceous waste, coated particle fuel from decommissioning of commercial, production, research reactors
- R & D to support future reactor operations, Gen IV system requirements

Operational Performance of Current UK Gas Reactors

- Graphite moderator degradation
  - Fast neutron irradiation
  - Radiolytic oxidation
  - High temperature
- Structural performance
  - How the graphite bricks respond
- Visual evidence
  - Understanding the microscale
  - Full of holes, cracks
  - Life limiting features
  - Predicting the macroscale performance

Typical Arrangement of an AGR Graphite Core

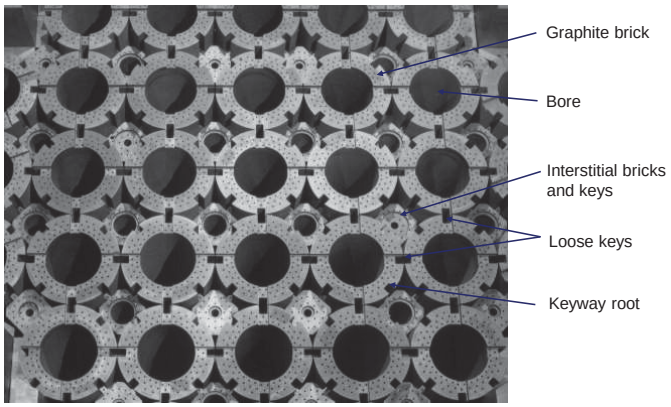

Analysis and Experiment

- Analysis of graphite components
  - Stress analysis of graphite bricks [1]
  - Statistical assessments of brick behaviour
  - Interactions of bricks in an array
  - Modelling crack propagation
- Mechanical testing of graphite components
  - Manufacturing cracked bricks
  - Pre-stressing, then investigating crack propagation
  - Internally stressed bricks
  - Dynamic testing
  - Brick slice tests
  - Key tests
  - Active laboratory facility

AGR Graphite Stress Analyses

- Issues
  - AGR bricks cracking
  - Crack propagation simulation
- Analysis Tools
  - Detailed finite element codes, FEAT, ABAQUS
  - Statistical analysis using SABRE, an EXCEL spreadsheet based tool
- Data availability
  - Relatively little data from Materials Test Reactors (MTR)
  - Component testing, bricks from virgin graphite
  - Mainly data from Magnox, some from AGR
  - NDT scan with eddy current, Investigation during outage, measure impedance – hence structure condition

Brick Cracking

- Bricks may crack due to internal hoop stresses
- Earlier in life the bore shrinks faster than periphery (a)
- Later in life the bore shrinks faster than the bore (b)
- Single and double brick cracking are possible

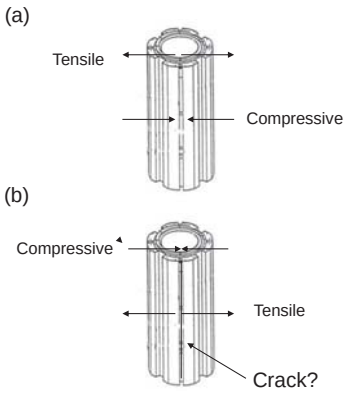

AGR Graphite Brick Stress Analyses – Field Variables

"Field variables define the ageing environment of the graphite components in the AGR cores."

Radiation: fast neutron damage, nuclear energy deposition (heating & ionisation)

Thermal-hydraulic: temperature, coolant flow, coolant composition

Weight loss: radiolytic oxidation

Note: neutron damage and nuclear energy deposition are often referred to loosely as "dose".

Stress analyses using finite element code

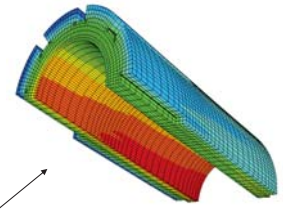

What are Field Variables needed for?

- Forecasts for AGR core Safety Cases
  - CCCA leg
  - Weight loss
- Correlation parameters for materials properties models
- Long term forecasts for PSRs and life extension
- For validation of ageing models against inspection data

Typical Stress Time History of an AGR Fuel Brick

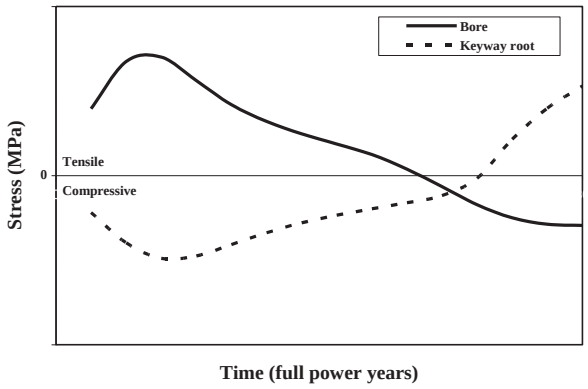

Validation

- How to validate the stress analyses when the in-reactor stress state is not measured?
- Good measurements of bore diameters from the Channel Bore Measuring Unit (CBMU)
- Can compare measured and calculated brick bore diameters

A Comparison of Calculated and Measured Bore Profiles

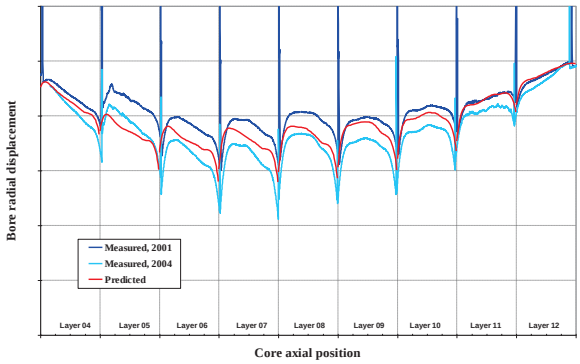

Mechanical testing of graphite core components

- Measuring load capacities/strengths/failure strains under specific loading configurations simulating plant conditions
- Data for safety cases usually through validation of finite element models or input to conventional calculations
- All testing:
  - Gilsocarbon graphite
  - At ambient temperature
  - Unirradiated graphite

Full Scale Core Brick Testing - Brick test rig

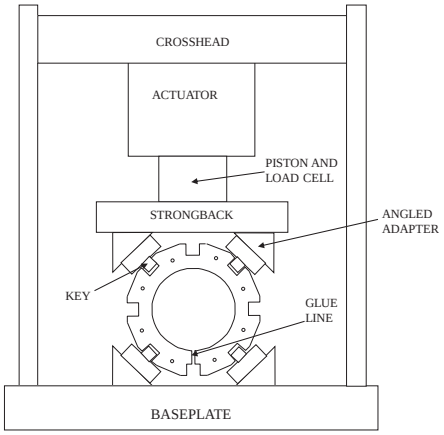

Graphite Dosimetry

- Work started with investigation of core restraint to support safety case arguments
- Aim to develop 3D solutions
- Carry-out extensive review to under-write ANSWERS MCBEND code
- Develop 3D method to provide dose distribution in any of the reactors
- Validation from extensive graphite data from Magnox reactors (much less available from AGR)
- Also validation from ASPIS facility cf DIMPLE reactor, Berkeley AGR
- Core Component Condition Assessment
- Novel methodology to calculate dosimetry, temperature, weight loss

Historical Approaches

- A variety of simplified 2D approaches have been used historically
  - Monte Carlo (MCBEND)
  - Lattice Physics (WIMS / CACTUS)
  - Kernel Methods (FAIRY)
- More recently the trend has been to use MCBEND
  - 2D distributions on a 1cm rectangular mesh
  - *Ad hoc* calculation of local 3D effects (e.g. FE end effects, grids & braces)
- Limitations:
  - 2D supercells, usually single channel or 2 x 2 arrays
    - Calculated for a generic brick – in an infinite reactor
    - Applies generic MCBEND result to each brick in the core based on local cumulative fuel irradiation
  - Not capable of representing asymmetry – e.g. core edge, vacancies, on-lattice control rods
  - Rectangular mesh does not accurately represent brick shapes

Revised Approach

- Use a reactor core octant model [2]
  - Enables generation of channel specific data
  - Can handle asymmetries (core edge, vacancies, control rods)
  - MCBEND “Fractal Geometry” options permit complex structures to be repeated
    - All bricks and channels can be modelled, methane holes can be included
- Model whole axial stack
  - Includes upper / lower reflectors and channel axial leakage
  - All axial features (FE gaps, grids/braces)
  - 3D source data: fuel element irradiations data from PANTHER Core Follow
- Extensive scoring mesh with radial, axial and angular subdivision for surveying groups of channels
- Advantages
  - Each channel/brick treated individually not as a generic component
  - Implicitly accounts for refuelling, reactor power changes, local perturbations due to control rods, neutron sources, burnable poisons etc.
- Disadvantages
  - Potential proliferation of the number of required calculations
    - Requires some simplification because of this to manage the large number

Dungeness B Core Octant Model

Planar section of 3D core octant model with brick scoring geometry inset:

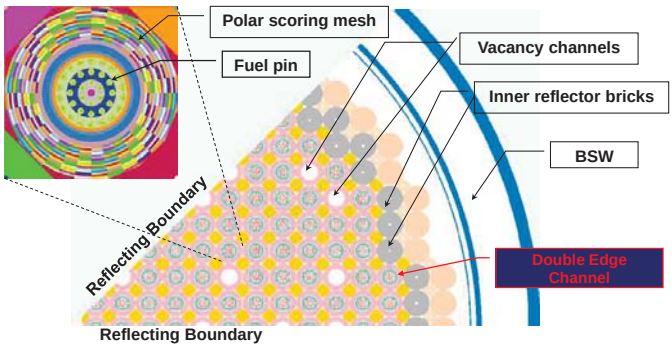

Typical Radial Distributions

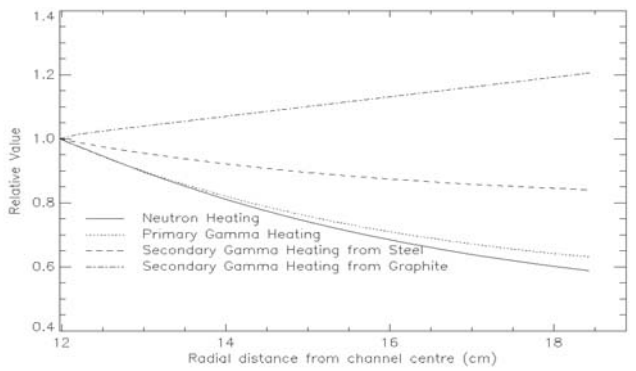

Separability Testing:
Dungeness Double Edge Channel: γ-Ray Energy Deposition

- Separability is confirmed for (r, θ)
- Core-octant models shown to be capable of producing results:
  - Four channels at once
  - In two overnight calculations
    [(r, z) and (r, θ)]
  - Per radiation source type (neutron / γ - ray)
  - Low stochastic uncertainties
  - Tabulated results give dosimetry data for each channel over its full height

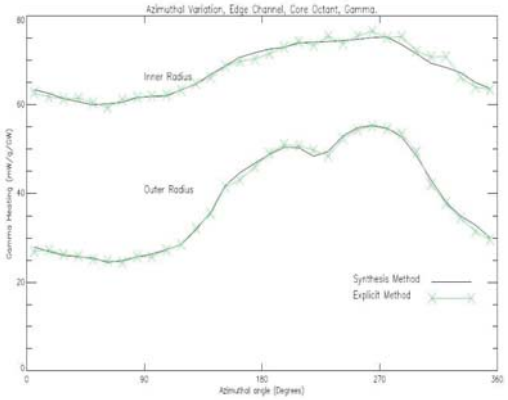

Validation Database

- Neutron Flux Measurements in Support of Dosimetry Calculations for an AGR

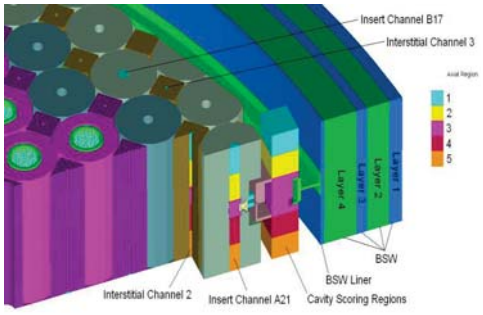

Validation Database (Cont.)

- Benchmarks: neutron and gamma radiation, range of materials
- AGR plant measurements: fast and thermal neutron edge & ex-core (both limited)
  - Neutron Flux Measurements in Support of Dosimetry Calculations for an AGR
  - Programme of work being undertaken to deploy two neutron flux measurement “stringers” within the side-core region of one of the Hunterston B reactors for the purpose of validating the MCBEND model. The design of the stringers and the determination of the preferred deployment locations have been informed by the use of detailed MCBEND flux calculations.
- Magnox flux measurements: neutron in-core (limited), neutron ex-core (extensive)
- BAGR (limited)
- Inter-code comparisons (limited)

R & D supporting Graphite Behaviour

- Design and assessment of Magnox & AGR graphite components relied on empirical data
- R & D is to better understand irradiation behaviour to design tests for selecting ‘best’ graphite for VHTR
- Research programmes carried out in Manchester and Cardiff:
  - Simulated neutron damage data using ion bombardment
  - Characterisation of unirradiated, ion irradiated and neutron irradiated graphite using advanced techniques (HRTEM, X-ray tomography, Raman spectroscopy) [3]
- Irradiated samples were managed through the AMEC (pre-cursor Serco) group at the active graphite laboratory in Risley – continuation at Manchester [4]

Active Laboratory Facility

- Used to characterise low level irradiated Magnox graphite samples.

Legacy Graphite Waste Management

- Scope
  - Retrieval, characterisation, treatment, disposal of various carbonaceous waste:
    - Irradiated graphite
    - Other carbonaceous structural materials
    - Coated particle fuels
- Reactor Decommissioning
  - Large scale commercial reactors
  - Production reactors
  - Prototype and research reactors

Legacy Graphite Waste Management (Cont.)

- UK
  - Magnox, AGR, Research reactors (GLEEP, DRAGON), Production reactors (Windscale piles, WAGR)
- International
  - RBMK (NB similar irradiation damage to gas reactors but not the oxidation problem)
- Options
  - Treatment and disposal
  - Burning
  - Recycling?
- Problem
  - Long-lived radioisotopes (^{14}C, ^{36}Cl, ^{129}I, ^{135}Cs, ^{79}Se, ^{99}Te in the graphite arising from irradiation processes in the graphite, activation of impurities, other materials transported to the graphite

Graphite Description and Relevant Issues

- Moderator graphite is a polycrystalline pitchcoke variety
- Shows some anisotropy
- Irradiation induced dimensional and mechanical property changes
- Wigner energy (WE)
  - Issue - extent of stored energy
- Oxidation by air
- Electrical conductor
- Will contain radio-nuclides from various processes
  - Issue – radionuclide content and transport

Safety Issues

Abnormal events in which graphite behaviour could:

- Lead directly to an uncontrolled release of radioactive material associated with the graphite itself or,
- Lead indirectly to an uncontrolled release of radioactive material from the graphite and adjacent structures

Hazards

- Internal Stresses, Dynamic and Static Loads
- Wigner Energy and Reactivity
- Leaching and Corrosion

Safety Measures and Monitoring During Decommissioning Stages

<u>Post Operational Clear Out (POCO)</u>

- No special considerations beyond steps to avoid any further possible mechanical damage to graphite

<u>Safe Storage</u>

- Long term environmental control
- Monitoring arrangements to assure control and warn of abnormal developments
- Fire prevention measures
- Maintenance of any measures already in place for extreme events (e.g. aircraft impact)

<u>Dismantlement</u>

- Routine radioactive working area establishment and control
- Minimisation of dust arisings and dust suppression methods
- PPE
- Control of routine discharges to the external environment and sources for external radiation exposure
- Graphite waste storage/conditioning hazards control.
- Interaction with disposal planning

Disposal of Coated Fuel

- Conventional UO2 fuel different from HTR fuel in that the coated-particles are directly embedded in the moderator (for pebble bed or prism fuel)
- Therefore spent fuel route strategy different
- Significant reduction of volume if the coated particles can be separated from the moderator matrix
- If reprocessing of fuel required, then separation of graphite, coatings, and fuel kernels is also required

Carbon-14 in the Biosphere – NDA RWMD

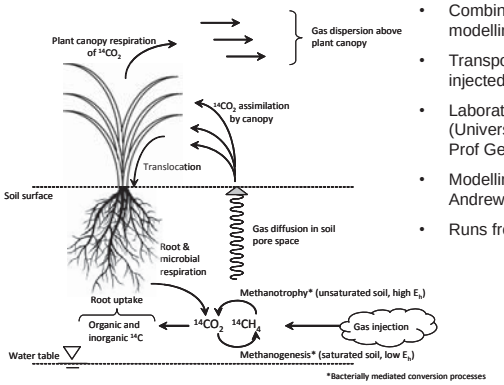

- Combined experimental and modelling programme
- Transport and fate of CH_4 injected into subsoil
- Laboratory and field experiments (University of Nottingham) – Prof George Shaw
- Modelling (Serco) – Andrew Hoch
- Runs from 2010 until 2013

^{14}C in Irradiated Graphite

- 81,000 tonnes of graphite in ILW and 15,000 tonnes in LLW
- Number of routes for ^{14}C production from irradiation of graphite:
  - $^{14}N(n,p)^{14}C$ reactions with nitrogen present as an impurity in fuels, moderators, coolants, and structural hardware
  - $^{17}O(n,\alpha)^{14}C$ reactions in oxide fuels, moderators and coolants and
  - $^{13}C(n,\gamma)^{14}C$ reactions in graphite moderators
- Uncertainty regarding:
  - the form of ^{14}C
  - its reactions
  - production of gaseous products
- Scoping study WAGR graphite
- Completed follow-up experiment BEP0 graphite
- Ongoing experiments Oldbury Magnox graphite

Graphite reaction vessel

References

1. C Jones, Predicting the Stresses and Deformations of Irradiated Graphite Moderator Bricks, Management of Ageing Processes in Graphite Reactor Cores Conference, Cardiff 2005
2. D.O Morgan, A.T. Robinson, D.A. Allen, D.J. Picton, D.A Thornton, S.E. Shaw, A Three-Dimensional Methodology for the Assessment of Neutron Damage and Nuclear Energy Deposition in Graphite Components of Advanced Gas Cooled Reactors, Reactor Dosimetry, 4th International Symposium, Journal of ASTM International, 2011
3. A Jones, G Hall, M Joyce, A Hodgkins, K Wen, T Marrow, B Marsden, Microstructural Characterisation of Nuclear Grade Graphite, Journal of Nuclear Materials, 381 (1-2), 152-157, October 2008
4. A J H Goddard et al, Safety & Performance for Innovative Reactors, Nuclear Future, Volume 03, Issue 5, September/ October 2007

Understanding Carbon-14 production in UK Magnox reactors by activation modelling and mass balance studies

Martin Metcalfe

Irradiation Damage and Formation in Nuclear Graphite, Joint meeting in conjunction with the FP7 Carbowaste programme, University of Manchester, 28 November 2012

Contents

Background

- Report on the progress being undertaken within NNL principally by Martin Metcalfe and Robert Mills, supported by Richard Jarvis, Anthony Banford and Nassia Tzelepi
- Nothing new about estimation of C14 inventories in nuclear plant
- Some excellent references in the open literature on origin of C14
- Current work recognises that fundamental processes are common to all reactor types, but C14 pathways and C14 inventories must be assessed by reactor type and often by individual reactor
- Work presented here relates to Magnox reactors, with focus on Oldbury and Wylfa and detailed analysis on Wylfa
- Objective: mass balance analysis to identify key factors determining C14 inventory

Mass balance model

- Consider two systems
  - Graphite core
  - Coolant circuits
- Graphite core model provides an input term for the coolant circuits model
- The graphite core model can be validated against measurements
- The coolant circuits model can be validated against recorded station discharge data

Mass balance model – graphite core

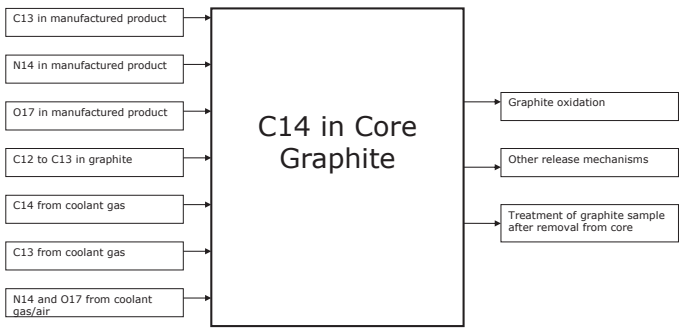

Mass balance model – graphite core

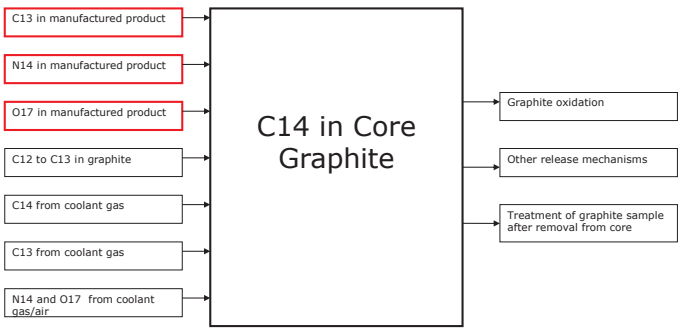

Mass balance model – graphite core

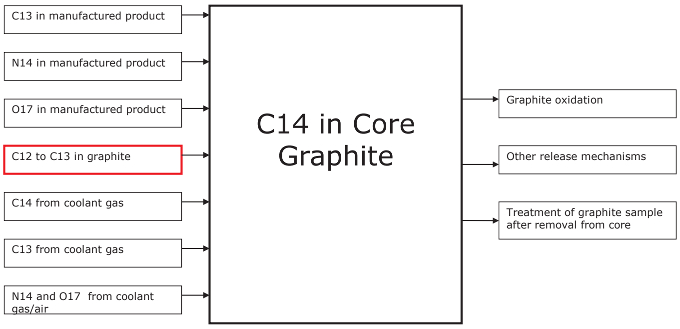

Mass balance model – graphite core

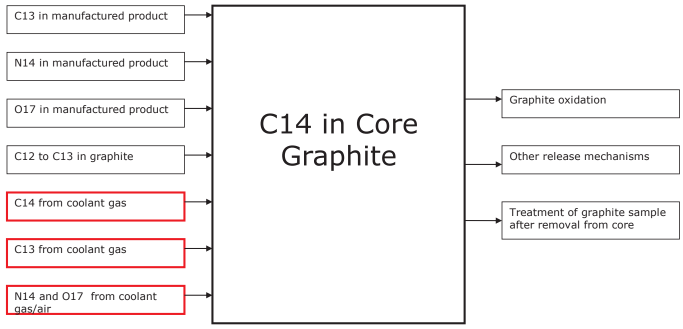

Mass balance model – graphite core

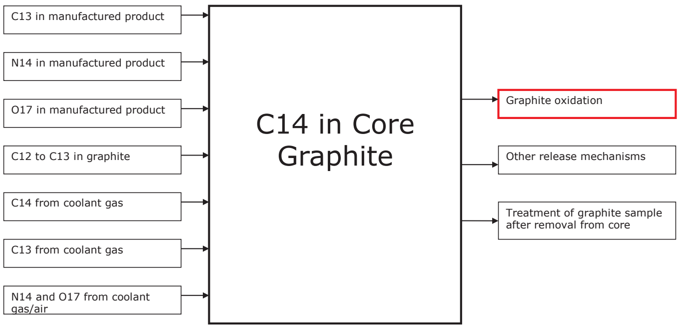

Mass balance model – graphite core

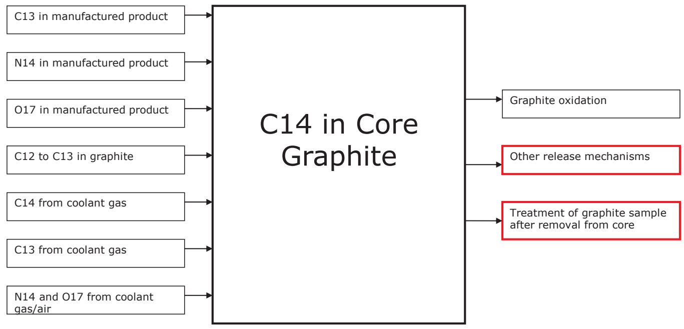

Mass balance model – graphite core

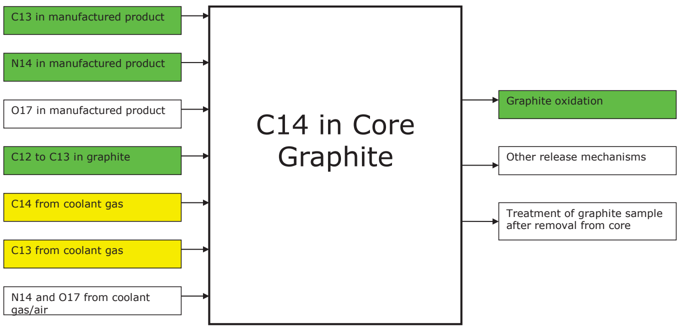

Mass balance model – coolant circuits

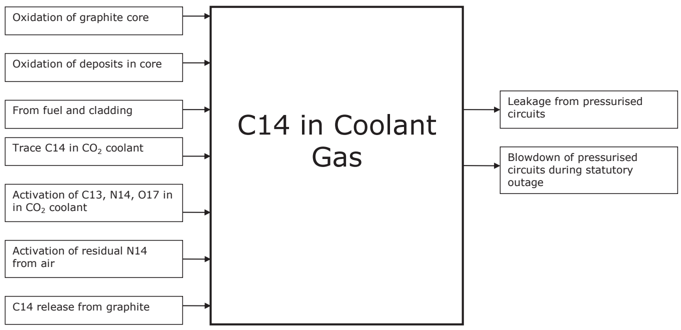

Mass balance model – coolant circuits

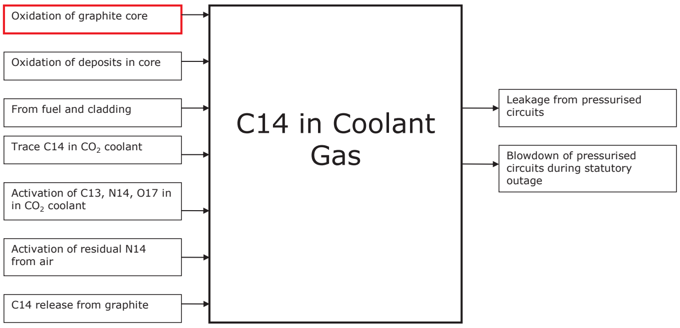

Mass balance model – coolant circuits

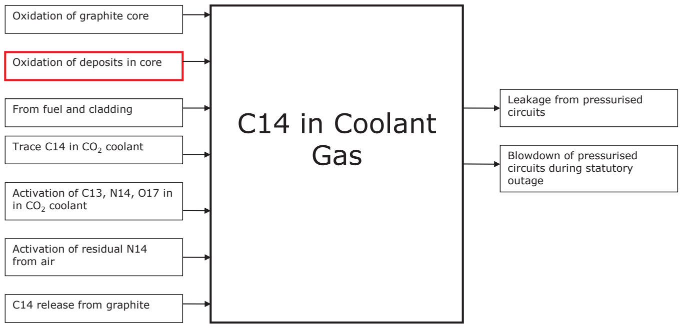

Mass balance model – coolant circuits

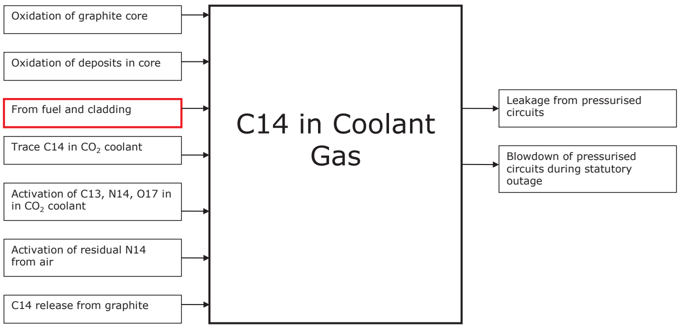

Mass balance model – coolant circuits

Global estimate of ^{14}C production, by reactor type

Reactor type	Component	Production estimate TBq/GWe-y	% of world generating capacity	Cumulated production to date (to the end of 2003) Estimated cumulative ^{14}C production PBq	Cumulated production to date (to the end of 2003) Available for release PBq
PWR	Fuel	0.72	65	2.6	
	Coolant	0.30		1.1	1.1
	Zircaloy + hardware[a]	0.38		1.4	
BWR	Fuel	0.73	23	0.9	
	Coolant	0.59		0.8	0.8
	Zircaloy + hardware[a]	0.51		0.7	
PHWR	Fuel	3.76	5	1.1	
	Coolant	0.38		0.1	0.1
	Moderator	27.0		7.6	7.6
Gas cooled	Fuel (Magnox/AGR/HTR)	6.1/1.8/0.17	7	1.0	
	Coolant (")	0.31/0.3/~0		0.06	0.06
	Moderator (")	10.8/3.4/3.1		3.8	
Grand total-reactors worldwide				21.1	9.6

PHWR: fuel includes our proposed value which includes production due to nitrogen impurities in fuel. Gas-cooled, given in the order of (Magnox/AGR/HTR). Values taken from (Liepins and Thomas, 1988) and (Braun et al., 1983).
[a] PWR and BWR updated values, based on Van Konynenburg (1994)—see text.

Taken from "Life cycle and management of Carbon-14 from nuclear power generation", Yim, M-S and Caron, F, Progress in nuclear energy 48, 2006

Mass balance model – coolant circuits

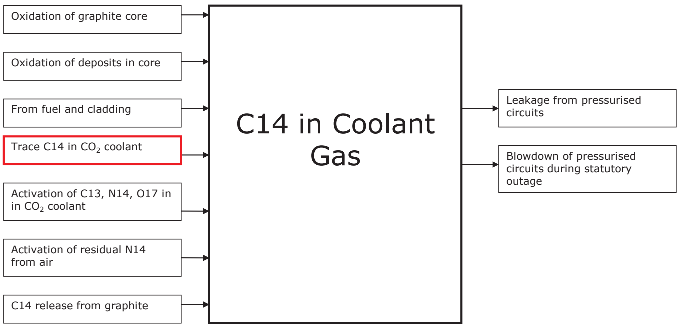

Mass balance model – coolant circuits

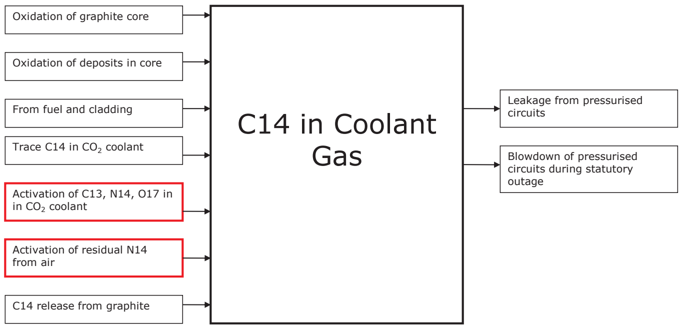

Mass balance model – coolant circuits

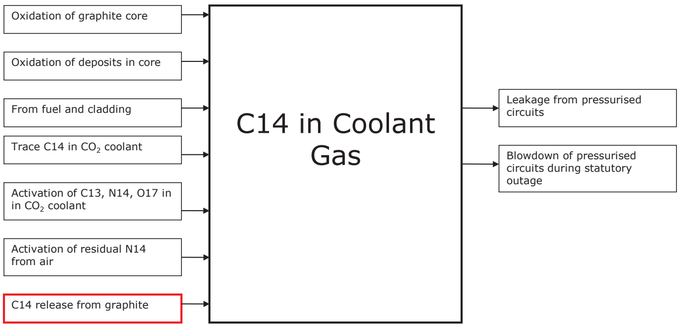

Mass balance model – coolant circuits

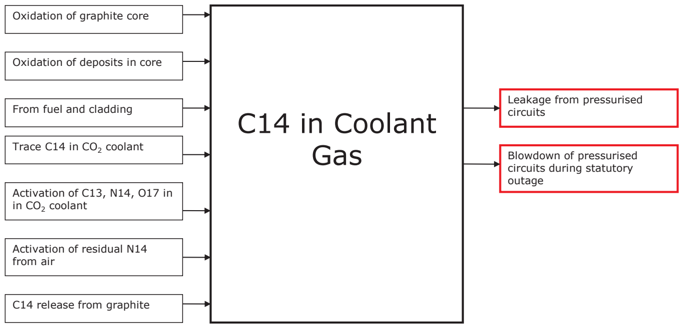

Mass balance model – coolant circuits

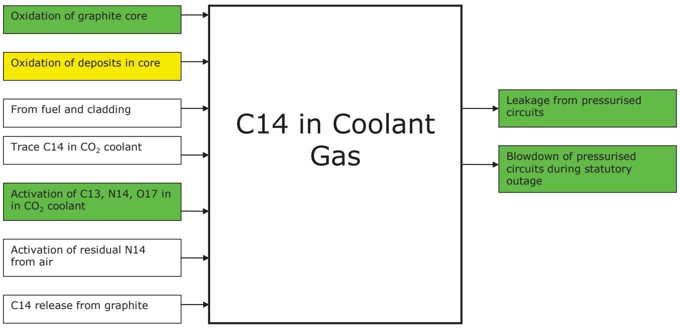

Activation modelling

Non-deterministic reactor physics code for modelling the behaviour of complex reactor geometries

NNL processing code to convert 172 group MCNP flux tallys to FISPIN libraries using TRAIL nuclear data to FISPIN cross-section

Standard UK Spent Nuclear Fuel inventory code for determining the irradiated nuclide inventory as a function of reactor power, initial enrichment, irradiation and cooling time (by solving the Bateman equations)

Activation modelling

Nuclear data issues – activation cross-sections for ^{14}C

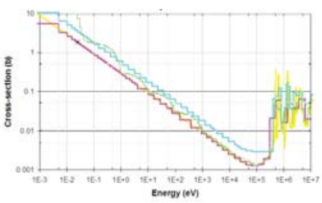

$^{14}N(n,p)^{14}C$

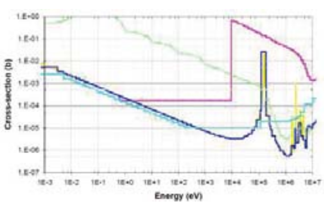

$^{13}C(n,\gamma)^{14}C$

TRAIL database (**pink**)
JEFF-3.1/A databse (**yellow**)
MCNPX-CINDER-2.6.0 database (**light blue**)
TENDL-2011 database (**green**)
Mughhabghab thermal value (black cross)
TRAIL based upon JEFF-3.1/A (**dark blue**)

Modelling Magnox reactor graphite activation

3D neutronic solution for the entire height of core with reflecting boundaries

- Run for specific sampling positions in the core and also to generate 3D maps of radionuclide build-up
- Fuel burn-up and replacement of fuel elements
- Graphite oxidation (weight loss) during irradiation
- Impurities and activation products immobile
- Verified against 2D WIMS calculations

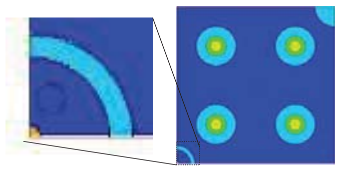

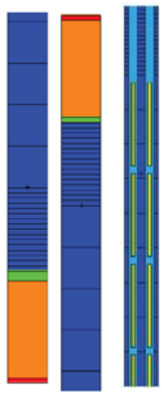

Modelling Magnox reactor graphite activation

NATIONAL NUCLEAR LABORATORY

Graphite oxidation

- Reduction in graphite density results in neutron spectra being shifted to slightly higher energies and a reduction in fission rate
- To maintain reactor power, the flux is increased by repositioning flux flattening absorbers and control rods
- For natural uranium fuel, production of Pu-239 together with fission product absorbers modifies flux
- As well as plutonium/fission product effect, decreasing graphite density increases the flux in each successive fuel cycle

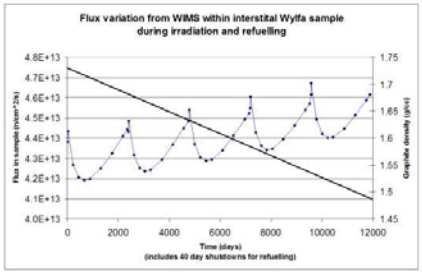

Activation calculations for specific specimens

NATIONAL NUCLEAR LABORATORY

- Full radionuclide fingerprints measured on 4 Magnox reactor specimens: 2 from Oldbury and 2 from Wylfa with known irradiation history.
- Specimens taken from installed carrier assemblies located in interstitial channel positions
- One Wylfa specimen skimmed prior to measurement (0.2 mm from surface)

Effect of $^{13}C(n,\gamma)^{14}C$ cross-section database

Specimen	Ratio of calculated/measured			
	Oldbury 1	Oldbury 2	Wylfa 1	Wylfa 2 (skimmed)
10 wppm N (old TRAIL)	19.9	15.9	208.0	77.0
10 wppm N (revised TRAIL)	0.3	0.3	3.5	1.3

Physics and element impurity input data critical to model predictions

C14 measurement versus prediction

NATIONAL NUCLEAR LABORATORY

- Model run with revised TRAIL database
- Two cases: N14 concentrations of 0 and 10 wppm

Specimen	Measured C14 activity (Bq/g)	Calculated C14 activity based upon natural impurities and zero contribution from N14 (Bq/g)	Difference between measured and calculated C14 activity (with zero contribution from N14) (Bq/g)	Calculated C14 activity based upon 10 wppm N and natural impurities (Bq/g)	N14 concentration required to align prediction with measurement (wppm)
Oldbury 1	2.80E+05	6.76E+04	2.12E+05	9.07E+04	92
Oldbury 2	3.78E+05	7.44E+04	3.04E+05	9.95E+04	121
Wylfa 1	2.72E+04	7.21E+04	-4.49E+04	9.55E+04	-19
Wylfa 2 skimmed	7.35E+04	7.21E+04	1.40E+03	9.55E+04	1

- For Oldbury samples, need around 100 wppm to align predictions with measurement
- For Wylfa samples, skimming has no effect and C14 can be aligned with C13 route alone

BUT ANALYSIS BASED UPON JUST FOUR RESULTS SO SHOULD BE TREATED WITH CAUTION

Contributions to C14 inventory from C13 and N14

NATIONAL NUCLEAR LABORATORY

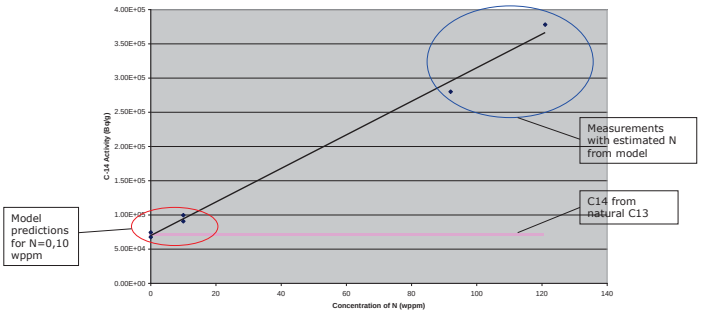

Whole core predictions of C14

NATIONAL NUCLEAR LABORATORY

- Analysis applied to Oldbury
- Whole core model based upon 2x2 model combined with a radial power distribution
- MCNPX/FISPIN approach repeated for 52 axial regions at:
  - central flattened zone
  - four positions in the region towards the edge of the core
  - the side reflector
- Model run until March 2011, with graphite density evolution estimated for each modelled region from start-up through to March 2011

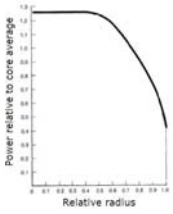

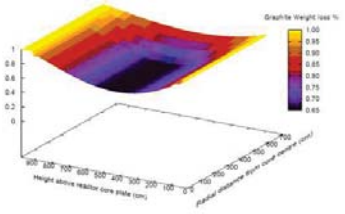

Whole core predictions of C14

NATIONAL NUCLEAR LABORATORY

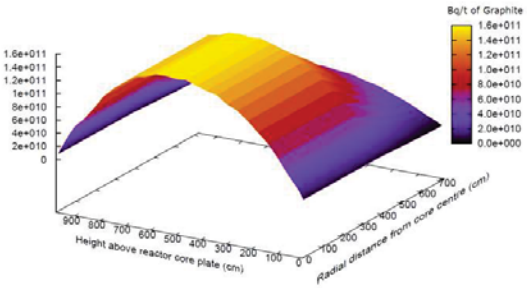

Whole core predictions of H3

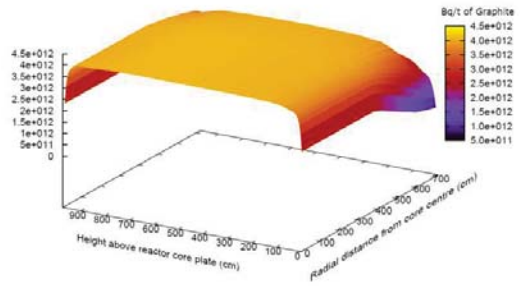

Whole core predictions

- No burn-out of C14 precursors (helped by C12 to C13 to C14 route)
- Calculations combined to give estimate of core average (Bq/t) of the important activities
  - 5.0E10 Bq/t assuming no contribution from N14
  - 7.8E10 Bq/t assuming 10 wppm N
- Predictions made for H3, C14, Cl36 and Co60
- Noteworthy that H3 activity is almost flat across the core due to almost complete conversion of every Li6 atom to H3 and He4 atoms.
- Work suggests that 65% of the C14 produced by activation of carbon (assuming 10 wppm N)

C14 predictions from the coolant

- Model run with revised TRAIL database
- C14 production rates (Bq/te/day) for the following cases:
  - pure CO2
  - CO2 with maximum allowable N impurity permitted in supply contract
  - CO2 with maximum measured N during operation
  - air
- Activation rates predicted for the 2x2 channel full height model taking account of fuel channel, interstitial and pore volumes.
- Model run at selected radial positions in the core so that a whole core average can be evaluated.
- In combination with contribution from graphite system, expected C14 discharge activities can be estimated and compared with actual reactor data
- C14 discharges from Wylfa Reactor 1 have been assessed for a 2-year period between statutory outages (September 2009 to August 2011)

C14 emissions from Magnox stations

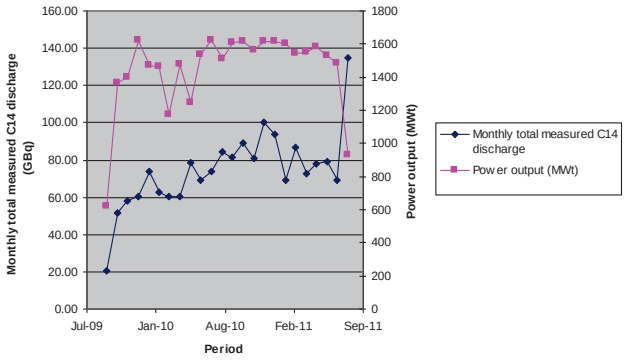

C14 emissions from Magnox stations

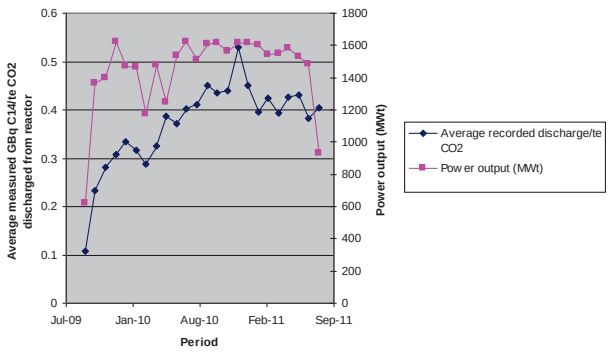

Concluding observations

- The mass balance of C14 has been separated into a graphite and coolant system
- The graphite system uses activation modelling to estimate C14 levels in the matrix which can be compared with measurement. Based upon this, a release rate into the coolant by radiolytic oxidation can be estimated using reactor oxidation data. The release rate can be cross-checked against monitored CO production rates.
- The coolant system uses activation modelling to estimate C14 levels arising from the gas. These can be combined with C14 released from the graphite.
- The equilibrium C14 level in the coolant during a sustained period of operation estimated from the model can be compared with actual monitored C14 discharges from the reactor.
- While it is not expected that the model estimates will align with measured discharges, the mass balance analysis will provide a tool for identifying key C14 pathways in a Magnox reactor.

Thank you for your attention

Any questions?

MODELLING OF ^{14}C PRODUCTION IN IRRADIATED GRAPHITE OF RBMK-1500 REACTORS AND COMPARISON WITH EXPERIMENTAL DATA

Ernestas Narkunas, Arturas Smaizys, Povilas Poskas

Lithuanian Energy Institute
Nuclear Engineering Laboratory

LITHUANIAN ENERGY INSTITUTE
Breslaujos str. 3, LT-44403 Kaunas http://www.lei.lt

Introduction

- There is one nuclear power plant in Lithuania – Ignalina NPP (INPP). It was shut down in the end of 2009;
- INPP has two Units with RBMK-1500 reactors. RBMK is water-cooled graphite-moderated channel-type power reactor;
- The core of one reactor Unit contains more than 1800 tons (more than 1100 m^3) of graphite. Graphite stack of RBMK reactor operates in the inert helium-nitrogen gas mixture atmosphere in order to avoid graphite oxidation and enhance cooling;
- After the final shutdown of the INPP, activated reactors graphite dismantling, handling, conditioning and disposal are an important parts of the decommissioning activities;
- One of the most important radionuclides generated in graphite is long-lived ^{14}C. This radionuclide may be generated through several different ways in RBMK reactor's graphite;

LITHUANIAN ENERGY INSTITUTE
Breslaujos str. 3, LT-44403 Kaunas http://www.lei.lt

Introduction (cont.)

- ^{14}C may be generated from activation of raw graphite material – carbon (through $^{13}C(n,\gamma)^{14}C$ reaction) and from activation of nitrogen impurities (through $^{14}N(n,p)^{14}C$ reaction);
- The production of ^{14}C from oxygen activation (through $^{17}O(n,\alpha)^{14}C$ reaction) is not significant for RBMK reactors (small reaction cross-section, low concentration of oxygen impurity and absence of oxygen in reactor cooling gas);
- The part of generated ^{14}C from the raw carbon activation may be modelled quite precisely as the quantity of carbon in graphite is almost invariant (comprises more than 99.9 % of mass);
- The part generated from nitrogen activation may be different depending on the initial nitrogen impurity content;
- Furthermore, the propagation of cooling gas (helium-nitrogen mixture) into graphite pores may additionally increase the quantity of nitrogen in graphite and consequently increase ^{14}C generation

LITHUANIAN ENERGY INSTITUTE
Breslaujos str. 3, LT-44403 Kaunas http://www.lei.lt

Neutron activation modelling

Generally, the numerical assessment of neutron activation consist of two steps:

- Modelling of the spatial and energy distributions of the neutron fluxes throughout the analyzed reactor component;

and then, using these modelled neutron fluxes

- Modelling of induced activity in that component using known concentrations of initial impurities and main chemical elements in the component's material

LITHUANIAN ENERGY INSTITUTE
Breslaujos str. 3, LT-44403 Kaunas http://www.lei.lt

A general modelling scheme and codes used

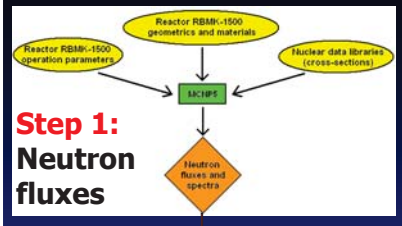

Step 1: Neutron fluxes

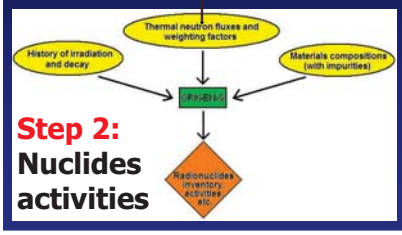

Step 2: Nuclides activities

MCNP 5 - a general-purpose, continuous-energy, generalized-geometry, time-dependent, coupled neutron/photon/electron Monte Carlo transport code, developed in Los Alamos National Laboratory (USA);

ORIGEN-S – a computer code from SCALE 5 codes system developed in Oak Ridge National Laboratory (USA). Code considers radioactive disintegration and neutron absorption and enables identifying isotopic content, activities and concentrations of activated material

LITHUANIAN ENERGY INSTITUTE
Breslaujos str. 3, LT-44403 Kaunas http://www.lei.lt

Part 1

DIFFERENT MECHANISMS OF ^{14}C PRODUCTION IN THE GRAPHITE OF RBMK-1500 REACTORS

Main data for neutron fluxes modelling

Various data of INPP Unit 1 RBMK-1500 reactor were used while developing MCNP model of the problem. These data are:

- ✓ geometrics of reactor components;
- ✓ materials compositions, temperatures and densities;
- ✓ reactor operation parameters and others

It was assumed that:

- ✓ FA consists of 2 bundles, with UO_2 fuel of average burnup of ~10 MWd/kgU with 2.4 % U-235 initial enrichment and 0.41 % Er_2O_3 absorber;
- ✓ coolant density in the central part of FC is 0.5 g/cm^3 while in the bottom and top FC parts it equals to 0.75 g/cm^3 and 0.25 g/cm^3 respectively;
- ✓ selected temperatures of described reactor components correspond to the conditions of fuel channel working on average power (~2.61 MW)

LITHUANIAN ENERGY INSTITUTE
Breslaujos str. 3, LT-44403 Kaunas http://www.lei.lt

View of RBMK-1500 reactor

(Modelled one lattice segment, periodic boundary conditions)

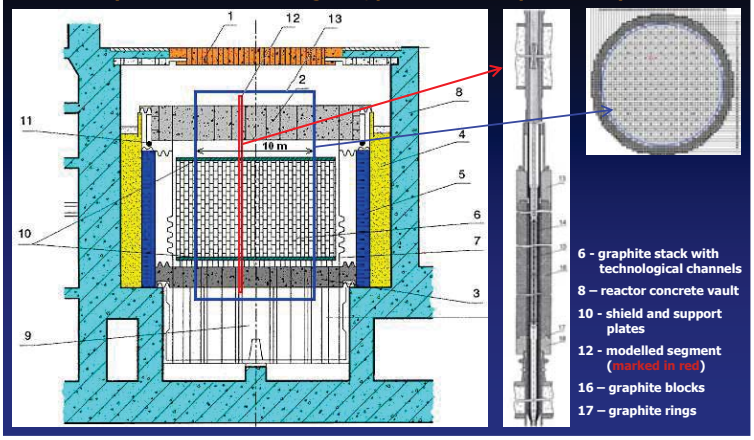

6 - graphite stack with technological channels
8 – reactor concrete vault
10 - shield and support plates
12 - modelled segment (marked in red)
16 – graphite blocks
17 – graphite rings

LITHUANIAN ENERGY INSTITUTE
Breslaujos str. 3, LT-44403 Kaunas http://www.lei.lt

Model of RBMK-1500 rector one lattice segment developed with MCNP code

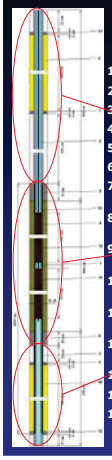

1 - FC central part;
2 - FC top part;
3 - FC bottom part;
4 - graphite blocks;
5 - steel shield plate;
6 - steel support plate;
7 - bottom steel plate of top metal structure;
8 - top steel plate of bottom metal structure;
9 - serpentinite filling of top metal structure;
10 - serpentinite filling of bottom metal structure;
11 - top steel plate of top metal structure;
12 - bottom steel plate of bottom metal structure;
13 - graphite rings;
14 - top fuel bundle;
15 - bottom fuel bundle

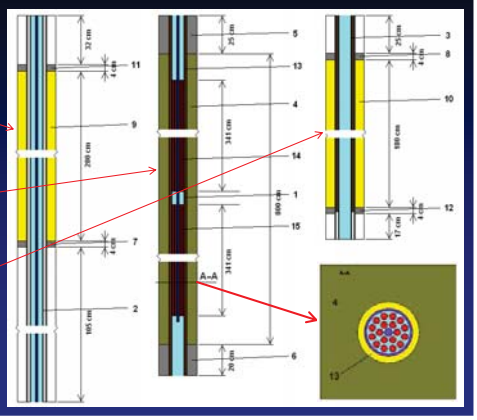

LITHUANIAN ENERGY INSTITUTE
Breslaujos str. 3, LT-44403 Kaunas http://www.lei.lt

Neutron fluxes modelling results

- ❑ **The estimated neutron fluxes with MCNP were grouped into the three energy groups:**
  - ✓ Thermal neutrons, with energies up to 0.625 eV;
  - ✓ Resonance neutrons, with energies in range of 0.625 eV – 1 MeV;
  - ✓ Fast neutrons, with energies above 1 MeV
- ❑ **Such neutron flux grouping allows direct input of the modelled fluxes from MCNP into the ORIGEN-S code for activation modelling**

LITHUANIAN ENERGY INSTITUTE
Breslaujos str. 3, LT-44403 Kaunas http://www.lei.lt

Modelled neutron fluxes in RBMK-1500 reactor's graphite blocks and rings

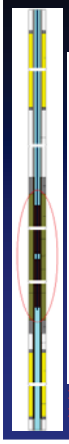

Axial distribution of modelled neutron fluxes

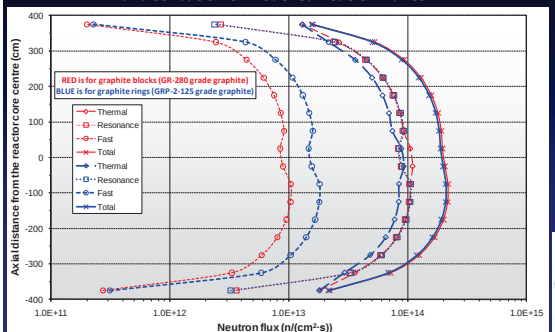

Radial distribution of modelled thermal neutron fluxes

- ✓ **Thermal and resonance neutron fluxes are dominant in the graphite structures**
- ✓ **Thermal neutron flux is slightly higher in the graphite blocks than in the graphite rings**

LITHUANIAN ENERGY INSTITUTE
Breslaujos str. 3, LT-44403 Kaunas http://www.lei.lt

Modelling of axial ^{14}C activity distribution

- ✓ Activation modelling was performed using already modelled neutron fluxes;
- ✓ Minimal and maximal concentrations of all impurities* (taken from published sources for graphite blocks and for graphite rings) were used when modelling axial ^{14}C activity distributions

* There is no published data on nitrogen impurity in GRP-2-125 grade graphite (graphite rings);
Minimal published nitrogen concentration in GR-280 grade graphite (graphite blocks) is 4×10^{-5} while maximal – 7×10^{-3} % (mass)

Modelled ^{14}C activity distribution in RBMK-1500 reactor's graphite blocks and rings

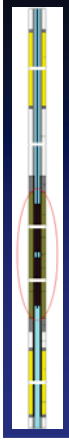

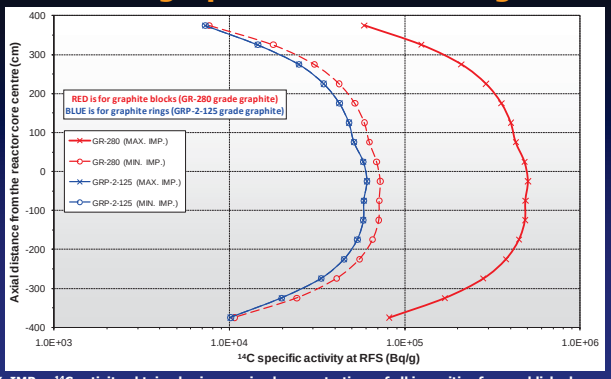

MAX. IMP. – ^{14}C activity obtained using maximal concentrations of all impurities from published sources

MIN. IMP. – ^{14}C activity obtained using minimal concentrations of all impurities from published sources

Modelling of ^{14}C activity dependence on nitrogen impurity content

Axial ^{14}C activity distributions in the graphite structures correspond to the thermal neutron flux distributions and maximal activities are induced in the central region

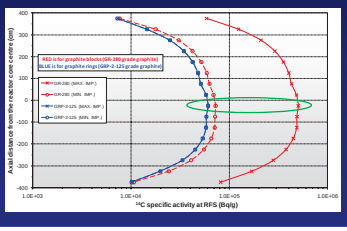

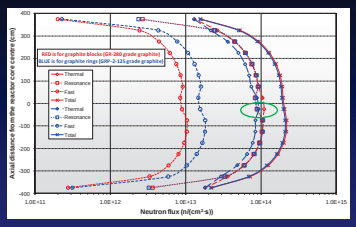

The influence of nitrogen impurity content on generated ^{14}C activities was analysed at the points with the highest axial ^{14}C activities

Modelling of ^{14}C activity dependence on nitrogen impurity content (cont.)

- ✓ Only nitrogen (and no other) impurity was taken into account;
- ✓ Several different modelling cases were developed with initial nitrogen impurity content ranging from 0 up to 0.05 % of mass;
- ✓ Theoretically possible nitrogen concentrations in the graphite pores were calculated according to the ideal gas law (pV=nkT) based on these parameters:
  - Nitrogen volumetric composition in cooling gas ranges from 5 to 100 %;
  - Cooling gas excess pressure ranges from 0.49 to 1.96 kPa;
  - Cooling gas temperature is 350 °C;
  - GR-280 grade graphite (blocks) porosity is 23 % (17 % are for open pores);
  - GRP-2-125 grade graphite (rings) porosity is 16 % (14 % are for open pores)

Theoretically calculated nitrogen content in graphite pores

Minimal and maximal calculated nitrogen concentrations in reactor RBMK-1500 graphite structures (due to the cooling gas penetration into the graphite pores) for any possible cooling gas composition and operating pressure:

Cooling gas excess pressure, kPa	0.49	1.96
Nitrogen volumetric fraction in cooling gas, %	5	100
Assuming, that cooling gas fills all open pores in graphite		
Nitrogen concentration in GR-280 graphite, % from initial graphite mass	2.8×10^{-4}	5.8×10^{-3}
Nitrogen concentration in GRP-2-125 graphite, % from initial graphite mass	2.1×10^{-4}	4.2×10^{-3}
Assuming, that cooling gas fills all pores in graphite		
Nitrogen concentration in GR-280 graphite, % from initial graphite mass	3.8×10^{-4}	7.8×10^{-3}
Nitrogen concentration in GRP-2-125 graphite, % from initial graphite mass	2.3×10^{-4}	4.6×10^{-3}

^{14}C activity dependence on nitrogen impurity content

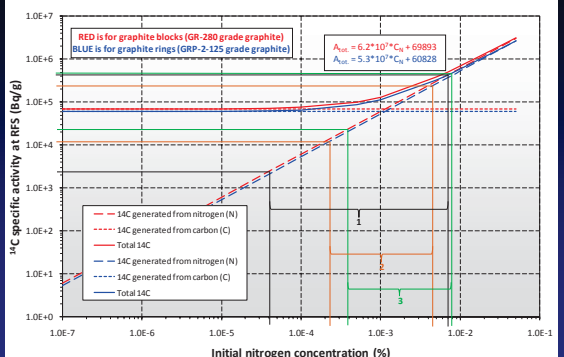

Interval 1 – nitrogen concentration in GR-280 grade graphite from published sources;
Interval 2 – calculated nitrogen concentration in GRP-2-125 grade graphite pores;
Interval 3 – calculated nitrogen concentration in GR-280 grade graphite pores

Maximal ^{14}C activity in the RBMK-1500 reactor graphite

Assuming:

- ✓ **Maximal initial nitrogen concentration of the GR-280 grade graphite (7×10^{-3} %) for both graphite grades;**
- ✓ **Maximal nitrogen concentrations from the cooling gases in the graphite pores:**
  - **7.8×10^{-3} % for GR-280 grade graphite;**
  - **4.6×10^{-3} % for GRP-2-125 grade graphite;**
- ✓ **All generated ^{14}C remains in the pores (not escaping into the cooling gases)**

for the very conservative case, at the places of maximal thermal neutron fluxes:

Maximal ^{14}C activity in the RBMK-1500 reactor graphite (cont.)

Total ^{14}C activity in the graphite blocks (GR-280) is about **9.9×10^5 Bq/g**, where:

- ✓ **~7 % comes from carbon activation;**
- ✓ **~44 % comes from nitrogen impurity activation in the graphite;**
- ✓ **~49 % comes from nitrogen activation in the graphite pores**

Total ^{14}C activity in the graphite rings (GRP-2-125) is about **6.8×10^5 Bq/g**, where:

- ✓ **~9 % comes from carbon activation;**
- ✓ **~55 % comes from nitrogen impurity activation in the graphite;**
- ✓ **~36 % comes from nitrogen activation in the graphite pores**

LITHUANIAN ENERGY INSTITUTE
Breslaujos str. 3, LT-44403 Kaunas http://www.lei.lt

Conclusions (part 1)

Finalising performed analysis of ^{14}C activity modelling in RBMK-1500 reactor graphite, several conclusion may be drawn:

- ✓ The activity of ^{14}C generated from carbon (raw graphite material) activation is in the order of 10^4 Bq/g;
- ✓ Generation of ^{14}C from activation of initial nitrogen impurities in graphite is linearly proportional to its quantity and at nitrogen concentration of ~1.1×10^{-3} % mass, ^{14}C generation from nitrogen activation equals the one from carbon;
- ✓ The very conservative estimation of possible nitrogen penetration from the cooling gasses into the graphite pores revealed, that nitrogen content in the graphite pores may be in the order of magnitude up to the 10^{-3} % of initial graphite mass, which is comparable to the maximal reported nitrogen impurity concentration in the graphite;
- ✓ ^{14}C generated from the activation of initial nitrogen impurity in the graphite and from the activation of nitrogen trapped in the graphite pores may significantly influence total generated ^{14}C activity in graphite

LITHUANIAN ENERGY INSTITUTE
Breslaujos str. 3, LT-44403 Kaunas http://www.lei.lt

Part 2

COMPARISON OF MODELLED AND MEASURED ACTIVITIES OF ^{14}C IN THE SAMPLES OF RBMK-1500 REACTOR GRAPHITE RINGS

LITHUANIAN ENERGY INSTITUTE
Breslaujos str. 3, LT-44403 Kaunas http://www.lei.lt

Experimental and modelling results of ^{14}C activities in the graphite of INPP RBMK-1500 reactor

- ✓ First experimental measurements of ^{14}C activity in the samples of irradiated graphite rings from the Ignalina NPP were performed within the frame of **EC 7FP CARBOWASTE** project;
- ✓ Measurements were performed by Institute of Physics (Lithuania, CPST) and results show, that ^{14}C activities in the graphite rings are higher than calculated ones (graphite rings, no nitrogen impurities);
- ✓ In order to have the agreement between measured and modelled activities, calibration of graphite activation modelling was performed, taking into account "explanatory" nitrogen impurity content;
- ✓ The "explanatory" concentration of nitrogen impurity was derived in "reverse" activation modelling way, i.e. the concentration of nitrogen impurity during modelling was altered until the modelled activity of ^{14}C matched best the measured ones

LITHUANIAN ENERGY INSTITUTE
Breslaujos str. 3, LT-44403 Kaunas http://www.lei.lt

Updated modelling using "explanatory" nitrogen impurity concentration for graphite rings

- ✓ As ^{14}C activity was measured in three different samples, corresponding to the three different heights along reactor axis, the best match was obtained by the help of least squares method;
- ✓ The calculated "explanatory" concentration was **13 ppm** of nitrogen. It gave the minimal sum of the squares of the differences between measured and modelled activities for all samples;
- ✓ This "explanatory" nitrogen concentration for graphite rings is in the range of reported concentrations for graphite blocks (0.4–70 ppm);
- ✓ Modelled ^{14}C activities using "explanatory" concentration of nitrogen impurity gave very good agreement with the measurement results – modelled activities fall in the range of measured ones taking into account measurement uncertainties

LITHUANIAN ENERGY INSTITUTE
Breslaujos str. 3, LT-44403 Kaunas http://www.lei.lt

Comparison of modelled ^{14}C activity in the graphite rings with the measured results

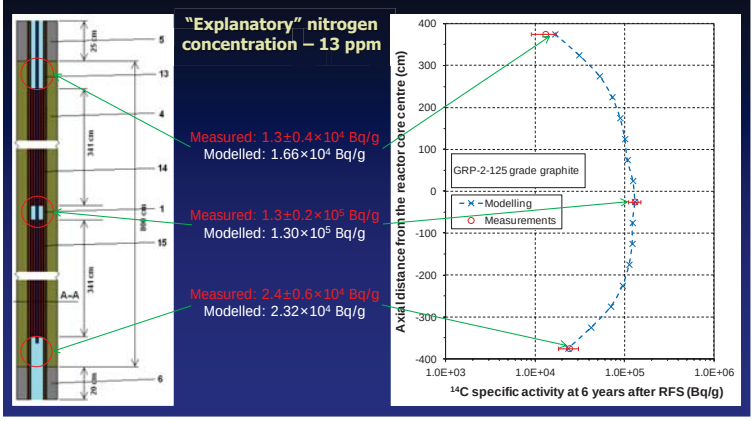

Conclusions (part 2)

Calibration of activation modelling was performed employing adjustment of initial nitrogen impurity content in order to get the modelled activities as close as possible to the measured ones. The performed evaluation shows that:

- ✓ Modelled ^{14}C specific activities in the graphite rings (using estimated "explanatory" nitrogen concentration) fall in the range of measured ones, taking into account measurement uncertainties;
- ✓ The calculated "explanatory" concentrations for nitrogen impurity in graphite rings fall in the range of reported concentrations for graphite blocks and in the range of calculated concentrations in the pores of graphite rings

Note:

The modelling presented here did not take into account two processes – possible release of nitrogen impurity or emerged ^{14}C radionuclide from the graphite component to the surrounding atmosphere and opposite process – uptake of ^{14}C radionuclide from the surrounding atmosphere !

LITHUANIAN ENERGY INSTITUTE
Breslaujos str. 3, LT-44403 Kaunas http://www.lei.lt

Thank you for your attention

Radionuclide inventory determination of UK irradiated graphite wastes

Greg Black

greg.black@postgrad.manchester.ac.uk

Dr. L. McDermott, Dr. A.N. Jones, Prof. B.J. Marsden

C. Fisher (ONR)

UK irradiated graphite legacy

- 38 major graphite moderated power production, plutonium production and research reactors in the UK
- represents a significant waste legacy arising from moderator, reflector and sleeves
- contains a variety of radionuclides as a result of neutron activation and contamination
- dismantling and management of radioactive graphite waste is an important issue in the UK

project objectives

- to inform future decommissioning, treatment and disposal options for graphite waste, through:
  - investigation of the origin, production pathways, location and final activity of radionuclides
- achieved by means of:
  - reactor simulation and activation modelling
  - experimental characterisation of virgin and irradiated graphite

14C production

- 14C significant radionuclide in waste
- risk of release and uptake in biosphere
- several potential production routes

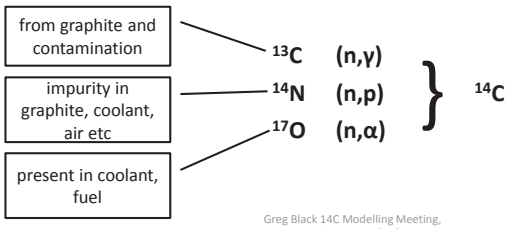

SIMULATION ROUTE

simulation process

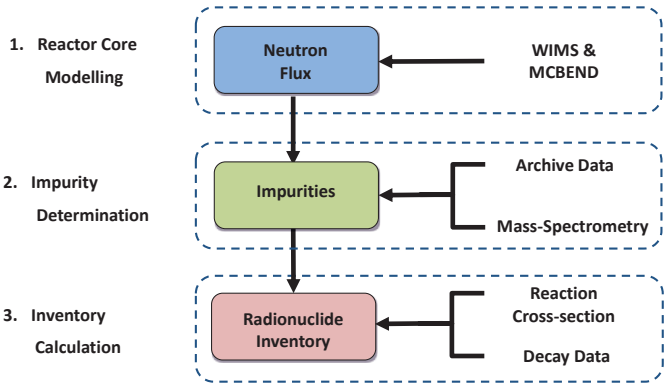

other factors influencing simulations

System	Parameter	Variable
Internal	Graphite	Impurities
		Radiolytic Oxidation / weight loss
Operating Environment	Flux	Changes to channel rating, flux profiles
		Loss of moderation
		Fuel composition
	Coolant gas	Composition
		Leakage during normal operation
		Leakage during outages/maintenance periods
Core	Other structural components	Fuel /clad
		Other channels
		Structural changes of the components

simulation stages

REACTORS OF INTEREST AND SAMPLE AVAILABILITY

Reactors of interest

- **BEPO**
  - Experimental- air-cooled reactor: 1948 - 68
  - Unique graphite grade- no virgin samples available
  - Natural and enriched Uranium, aluminium cladding
  - Multiple trepanned samples available

- **Magnox (PGA)**
  - Power/plutonium production - CO_2 cooled
  - Virgin PGA available
  - Natural U-fuel encased in Magnesium alloy
  - Trepanned samples from Wylfa and Oldbury

- **AGR (Gilsocarbon)**
  - Power reactors - CO_2 cooled
  - Virgin Gilsocarbon available
  - Enriched fuel encased in stainless -steel/graphite
  - Trepanned samples from Hinkley Point B

Oldbury nuclear power station

- Operation:
  - Magnox design
  - 2 reactors
  - commissioned 1967- 2012
- Graphite:
  - bottom reflector- PGB
  - top & side reflector- PGA
  - moderator- PGA
- Reactor:
  - 64 columns
  - 9.8m (height) by 14.2m (width)
  - 3308 fuel channels
  - 8 fuel elements per channel

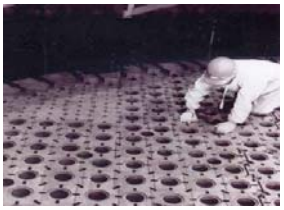

installed carrier and samples

Oldbury Pot 634	
Location	**Channel S77, R2**
Irradiation time	**1967 - 2005**
Irradiation Temp	**543 K**
Adjacent Fuel Dose	**52827 MWd/t**
Dimensions	**15 x 4 mm**
No. of samples	**24**

INVENTORY MODELLING

source description- WIMS

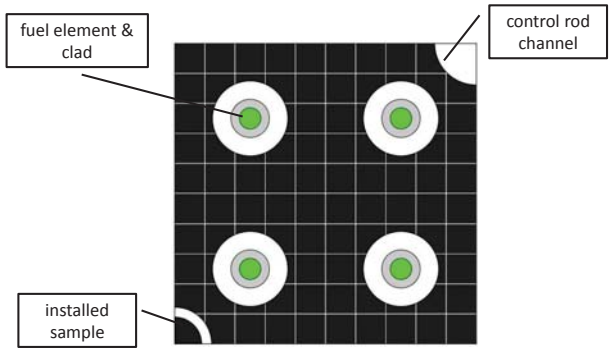

flux modelling- MCBEND

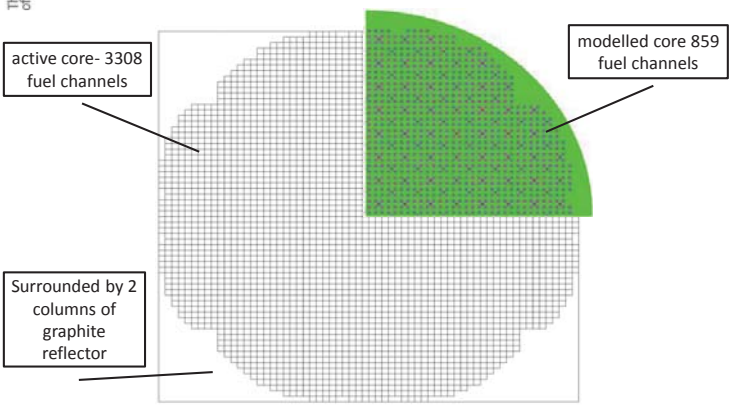

flux modelling- MCBEND

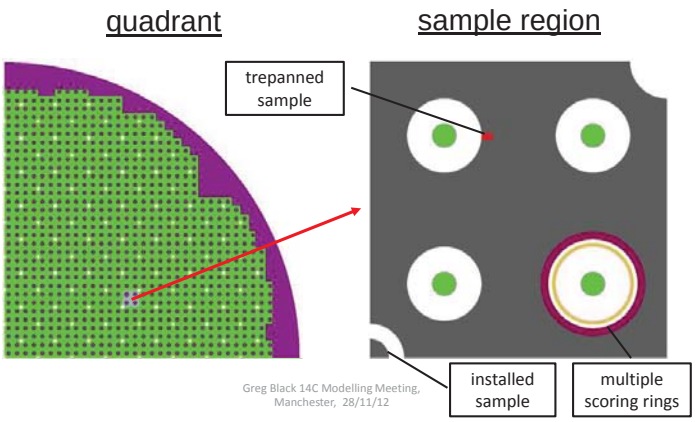

flux modelling- MCBEND

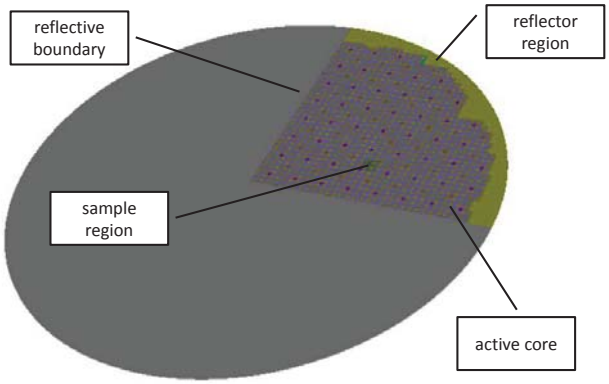

inventory calculation- FISPACT

- FISPACT-2007 neutron activation software developed by UKAEA
- Uses EAF-2007 database:
  - 65,565 neutron reaction cross-sections
  - Decay data for 2,231 radionuclides
- Takes into account operational and shutdown times
- Can include periods of increased or decreased flux
  - operational changes towards end of plant life
- Calculates end of life radionuclide inventory and production pathways

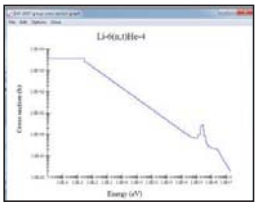

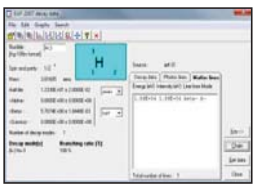

EXPERIMENTAL CHARACTERISATION

14C inventory determination

- **Thermal analysis has been used as a methodology for ^{3}H and ^{14}C determination**
  - 0.5g of i-graphite was placed in a combustion boat and analysed in a Carbolite® MTT Furnace
  - The combustion furnace utilises a copper oxide catalyst to promote ^{3}H and ^{14}C removal during heating under air/oxygen conditions
  - HTO and $^{14}CO_2$ which is subsequently trapped in the bubbler system for analysis using liquid scintillation counting (LSC)

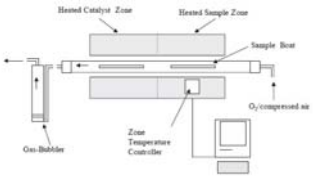

Round Robin Data Comparison

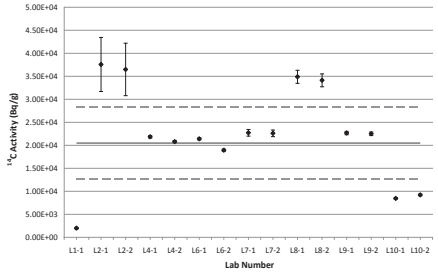

- The success and accuracy achieved within the Round Robin Test gave confidence in the determination of ^{3}H and ^{14}C by thermal analysis
- Thermal analysis using a carbolite® furnace is considered a suitable technique for ^{3}H and ^{14}C analysis in i-graphite

Isotopic distribution

- **Uneven distribution of isotopes within all i-graphite**
- **Determination of this distribution using autoradiography**
  - Amersham Typhoon 9410
  - Phosphorous storage films
  - Uniformity ± 5% over entire scan area
  - Pixel accuracy ± 0.15%
  - Exposure films are reusable

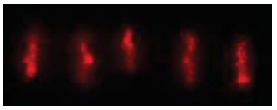

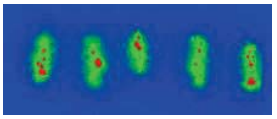

Oldbury samples

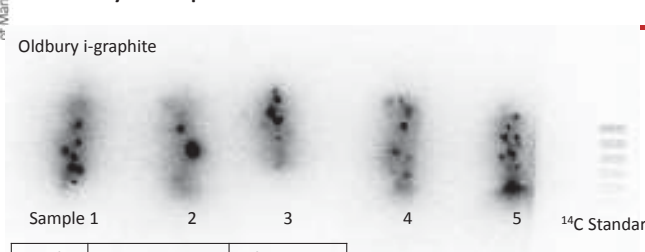

Sample	Average Intensity	Std Deviation
1	1521	1215
2	1408	842
3	1700	1476
4	1292	410
5	1695	667

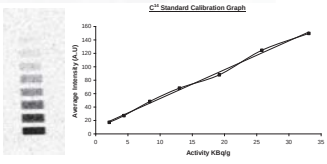

RESULTS

14C results

	Experimental		Simulation	
sample	Activity (Bq/g)	Uncertainty (%)	Activity (Bq/g)	C/E
Oldbury	6.36×10^4	10	5.02×10^4	0.79

- Comparison of experimental and simulated results for Oldbury installed samples
- Experimentally determined using thermal analysis
- 'C/E' represents the 'Calculated/Experimental' results, a precise match would result in a C/E value of 1.0

14C production pathways

10ppm N

sample	Production Pathway	Percentage of total
Oldbury	$^{13}C(n, \gamma)\ ^{14}C$	51.41
	$^{14}N(n,p)\ ^{14}C$	48.57

reaction cross-sections- EAF2010

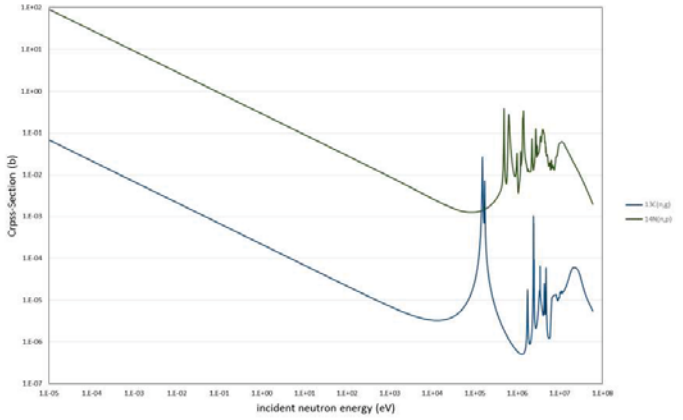

13C (n,γ) 14C from JANIS

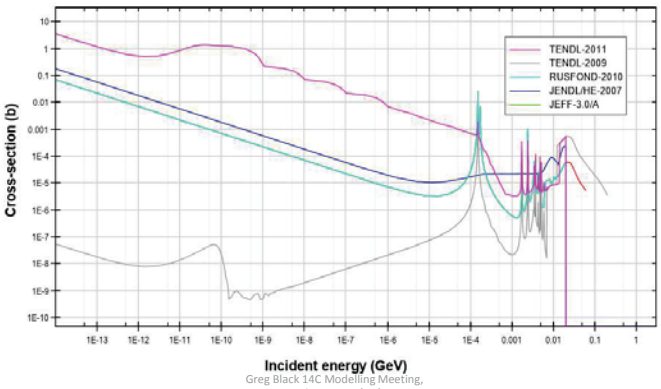

TENDL-2009 13C(n,γ)14C from JANIS

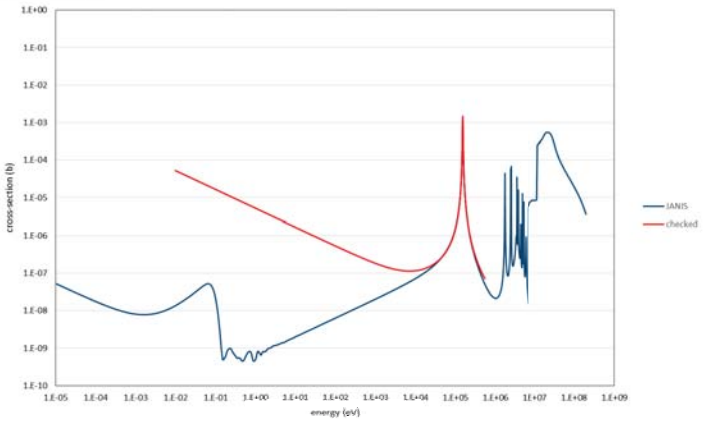

Impurity concentration- Nitrogen

In Graphite (ppm)	
Magnox	>10
AGR	>10
BEPO	no data

- White, I. F., Smith, G. ., Saunders, L. ., Kaye, C. ., Martin, T. ., Clarke, G. ., & Wakerley, M. . (1984). *Assessment of management modes for graphite from reactor decommissioning.*
- Anglo Great Lakes. (n.d.). *Anglo Great Lakes- UK Nuclear Graphite Impurities.*

Coolant composition (vpm)		
	Magnox	AGR
carbon monoxide (%)	1.0 – 1.5	1.0 – 1.5
hydrogen	25 – 45	no data
methane	< 10	150-300
water	< 1	300
argon	5	<5
nitrogen	500	<500

- Nuclear Electric PLC. (1990). *AGR Design and Technology Course.*
- Nuclear Electric PLC. (1990). *Magnox design and technology course.*

production pathways- ^{14}C

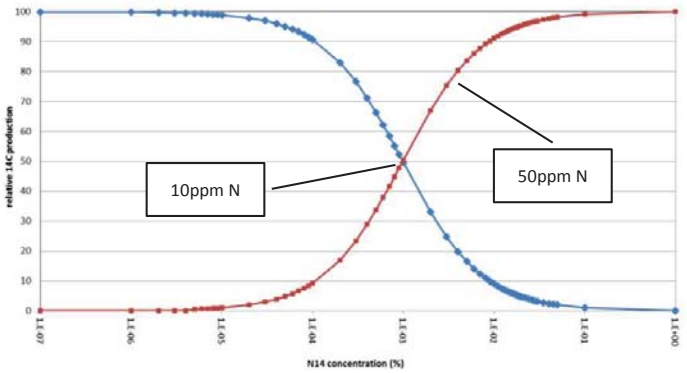

CONCLUSIONS & FUTURE WORK

Greg Black 14C Modelling Meeting, Manchester, 28/11/12

conclusions & future work

- Oldbury:
  - models for any position and sample geometry
  - burnup and density change included
- other reactors:
  - models for BEPO, Wylfa & Hinkley-B
  - i-graphite samples from each reactor
  - comparison study underway
- future work:
  - operational data to increase accuracy
  - sensitivity studies of impurity data
  - scalability from sample to whole core
  - comparison of results with WIMS-FISPIN

Greg Black 14C Modelling Meeting, Manchester, 28/11/12

acknowledgements

research funded by ONR as part of the CARBOWASTE project: FP7-211333

thank you to the following organisations for their support

Greg Black 14C Modelling Meeting, Manchester, 28/11/12